



2

2022

# JOURNAL OF NEW TECHNOLOGIES IN ENVIRONMENTAL SCIENCE

No. 2 Vol. 6 ISSN 2544-7017 www.jntes.tu.kielce.pl Kielce University of Technology

## CONTENTS

Bogdan TSELEN, Georgiy IVANITSKY, Anna NEDBAYLO, Nataliya RADCHENKO <b>PROSPECTS FOR THE USE OF CAVITATION MECHANISMS IN ORDER TO REDUCE THE CONSUMPTION OF NATURAL WATER IN MUNICIPAL ENERGY</b> .....	53
Borys BASOK, Denys DEREVINKO, Nataliia BESPALA, Ihor BOHOIKO <b>FEATURES OF COMPLEX ASSESSMENT OF ENERGY CONSERVATION MEASURES IN BUILDINGS</b> .....	59
Oleksandr SIGAL, Dmytro PADERNO, Nataliia NIZHNYK <b>POSSIBILITIES FOR THE PRODUCTION AND USE OF HYDROGEN AS A FUEL IN EXISTING BOILERS</b> .....	65
Dagmara KOTRYS-DZIAŁAK, Katarzyna STOKOWIEC <b>TEMPERATURE DISTRIBUTION ANALYSIS ON THE SURFACE OF THE RADIATOR WITH AN INFRARED CAMERA AND THERMOCOUPLES</b> .....	67
Viacheslav MYKHAILYK, Tetiana KORINCHEVSKA, Valery DAKHNENKO <b>TORREFACTION OF COMPOSITE BIOFUEL IN THE ATMOSPHERE OF ITS OWN GASEOUS ENVIRONMENT</b> .....	75

**Editor-in-Chief:**

prof. Lidia DĄBEK – Faculty of Environmental, Geomatic and Energy Engineering,  
Kielce University of Technology (Poland)

**Associate Editors:**

prof. Anatoliy PAVLENKO – Faculty of Environmental, Geomatic and Energy Engineering,  
Kielce University of Technology (Poland)

**Board:**

prof. Anatoliy PAVLENKO – Kielce University of Technology (Poland)

prof. Lidia DĄBEK – Kielce University of Technology (Poland)

prof. Hanna KOSHLAK – Kielce University of Technology (Poland)

**International Advisory Board:**

prof. Boris BASOK, academician of the NAS of Ukraine – Institute of Engineering Thermophysics National  
Academy of Sciences of Ukraine

prof. Mark BOMBERG – McMaster University (Canada)

prof. Jan BUJNAK – University of Žilina (Slovakia)

prof. Valeriy DESHKO – National Technical University of Ukraine “Igor Sikorsky Kyiv Polytechnic Institute” (Ukraine)

prof. Ejub DZAFEROVIC – International University of Sarajevo (Bosnia-Herzegovina)

prof. Andrej KAPJOR – University of Žilina (Slovakia)

prof. Engvall KLAS – KTH (Sweden)

prof. Vladymir KUTOVOY – Harbin Institute of Technology (China)

prof. Ladislav LAZIĆ – University of Zagreb (Croatia)

prof. Zhang LEI – Faculty of Thermal Engineering, CUPB University of Oil and Gas (China)

prof. Milan MALCHO – University of Žilina (Slovakia)

prof. Violeta MOTUZIENĖ – Vilnius Gediminas Technical University (Lithuania)

prof. Łukasz ORMAN – Kielce University of Technology (Poland)

prof. Jerzy Z. PIOTROWSKI – Kielce University of Technology (Poland)

prof. Miroslav RIMÁR – Technical University of Košice with a seat in Prešov (Slovakia)

prof. Ibragimow SERDAR – International University of Oil and Gas (Turkmenistan)

[www.jntes.tu.kielce.pl](http://www.jntes.tu.kielce.pl)

[jntes@tu.kielce.pl](mailto:jntes@tu.kielce.pl)

The quarterly printed issues of Journal of New Technologies in Environmental Science are their original versions.  
The Journal published by the Kielce University of Technology.

ISSN 2544-7017

Doi: 10.53412

© Copyright by Wydawnictwo Politechniki Świętokrzyskiej, 2022



Bogdan TSELEN, Georgiy IVANITSKY

Anna NEDBAYLO, Nataliya RADCHENKO

*Institute of Engineering Thermophysics of NAS Ukraine*

*2a Marii Kapnist Str., Kyiv, 03057, Ukraine*

Corresponding author: ittf\_tds@ukr.net

Doi: 10.53412/jntes-2022-2-1

## PROSPECTS FOR THE USE OF CAVITATION MECHANISMS IN ORDER TO REDUCE THE CONSUMPTION OF NATURAL WATER IN MUNICIPAL ENERGY

**Abstract:** *The paper discusses the existing methods of neutralizing condensate among which the most effective method of hydrodynamic cavitation is determined. To implement the effects of hydrodynamic cavitation, it is proposed to use the way of discrete – pulsed energy input, which allows neutralization by degassing condensate of natural gas combustion products.*

*Based on the created universal mathematical models of the dynamics of single steam-gas bubbles and the ensemble of bubble dynamics, numerical modeling of the growth of steam-gas bubbles in condensate was carried out. Within the framework of the mathematical model of the dynamics of the ensemble of bubbles, an analytical study of the evolution of the unit of steam-gas bubbles to achieve a critical value of the gas content in them was carried out.*

*It has been experimentally proven, the effectiveness of the proposed method, in particular, has been established that the main amount of carbonic acid from both flue gas condensate and model liquid is removed within two minutes of processing. The obtained data prove that an increase in the pH of the treated condensate corresponds to the pH of distillate, which indicates the complete removal of carbonic acid. The implementation of the proposed method of neutralizing condensate will create conditions for improving the environment. This is achieved by reducing the amount of effluent and rational use of water resources by reducing the need for natural water.*

**Keywords:** *cavitation, acidic condensate, neutralization*

### Introduction

Condensate formed during the combustion of natural gas in boilers equipped with a system of deep utilization of the heat of flue gases at municipal energy enterprises is not reused. As a rule, after chemical neutralization, it enters the wastewater of enterprises. Neutralization of condensate is necessary due to the low pH value, which is due to the high content of carbonic acid (approximately 70 mg/l of carbon dioxide). For this purpose, methods of neutralization with chemical reagents and neutralization using mass transfer processes are used. The disadvantage of chemical neutralization is a significant contamination of neutralized condensate with neutralization reaction products and the impossibility of its further reuse. Common mass exchange processes (decarbonization, thermal and vacuum deaeration) are not used to neutralize condensate due to high energy costs or due to insufficient carbon dioxide extraction. Given that from 1 MW of thermal power of the boiler unit, as a rule, up to 140 l/h of condensate is formed, this leads to the formation of a significant amount of it, so it is advisable to consider the possibility of reusing condensate in order to reduce natural water consumption and wastewater emissions.

## Analysis of existing research

Analysis of many sources, including work [1-3] showed that the neutralization of acidic condensate with chemical reagents can be implemented in equipment using a solid reagent, by liquid neutralization, as well as using reagents based on neutralizing amines.

The principle of equipment operation based on the use of solid reagent involves passing acid condensate through a layer of neutralizing reagent. The use of such equipment does not imply the regulation and control of stable values of the hydrogen indicator. It is advisable to use it for boilers with a capacity of up to 1000 kW. The principle of operation of the liquid neutralization equipment involves the addition of a dosed amount of liquid reagent to the acidic condensate. The use of automated dosing and control systems makes it possible to obtain a stable final value of the pH indicator, as well as the possibility of its regulation. Such equipment is economically feasible for boilers with a capacity of more than 1000 kW. The use of special chemicals based on neutralizing amines to adjust the hydrogen index of water is economically impractical due to their too high cost.

Neutralization of acidic condensate using mass exchange processes can be carried out on absorbent-type devices. Their work is based on the extraction of dissolved carbon dioxide as a result of contact with air. Its course is due to a significant number of interdependent factors that can change over a wide range. For example, as indicated in the article [4] the solubility of carbon dioxide in water depends on its temperature, which changes during the decarbonization process. The method is one of the most complex mass transfer processes in the preparation of water in the heat and power industry. Existing decarbonizers are divided into two groups – countercurrent and direct-flow.

The countercurrent decarbonizer is a nozzle apparatus with air supply by a fan from the bottom. Decarbonizers of this design have been used for more than 50 years and are obsolete as evidenced by the article data [5]. The disadvantage of devices of this type is their impressive dimensions, high cost, complexity in maintenance and repair, as well as the need for individual design.

Among direct – flow decarbonizers, ejection devices and direct – flow spray heat and mass transfer device are common. The use of water – jet ejectors is limited due to the low values of the permissible initial concentration of carbon dioxide (up to 20 mg/kg). Direct-flow ejections heat and mass transfer devices can have an ejection coefficient of about 1000, however, the productivity can be from units to hundreds of m<sup>3</sup>/h·m. Common disadvantages of devices of this type are large dimensions and weight, and therefore they have not found wide application.

Among modern alternative methods, it is worth noting acoustic, in which high-frequency ultrasonic generators are used. Their effectiveness lies in the fact that they ensure the fastest possible removal of free gas from the liquid, which is contained in gas bubbles. The degassing of the liquid occurs due to the fact that a significant part of the dissolved gas under the influence of ultrasonic vibrations passes into the bubbles, which subsequently exit the liquid through the phase separation surface. Their advantage lies in the possibility of degassing almost any liquid. However, now these methods are not widely used due to significant specific energy costs.

In recent years, more and more attention has been paid to the possibilities and advantages of using hydrodynamic cavitation in various fields. Numerous studies and implementation of the obtained results in various fields of production have shown that hydrodynamic cavitation should be considered as a significant alternative to acoustic cavitation in the direction of increasing productivity and reducing specific energy consumption.

## Problem formulation

Taking into account the previous experience of scientific work and the shortcomings and complexities of existing equipment, the authors proposed a new alternative method of reagent – free neutralization of condensate. The research carried out within the framework of the project "Improving the efficiency of technology for reducing nitrogen oxide emissions by recirculating flue gases in boiler installations of municipal and industrial energy" (Agreement No. 904 of 04.01.22).

It is method based on the use of physical effects on the treated environment and avoids the addition of chemical reagents, characterized by low specific energy and material costs. The proposed method was initiated on the basis of fundamental research within the framework of the scientific direction of discrete – pulse energy input (DPEI) into dispersed systems and is covered in the work [6]. It includes the use of mechanisms such as high – frequency hydrodynamic vibrations, accompanied by high circumferential speed and shear stresses, as well as cavitation phenomena and transient phase transitions. Removal of carbonic acid from condensate in this way will avoid chemical neutralization and obtain practically degassed desalinated water. Then it can be used to prepare water to power the boilers, bypassing the stage of water softening, as well as for other technological needs.

To accomplish this task, it is necessary:

- to carry out previous modeling of the process of growth of gas-steam bubbles in condensate;
- to experimentally establish the regularity of the influence of cavitation mechanisms on the pH of condensate and investigate its stability over time.

## Materials and methods

To carry out numerical modeling, universal mathematical models of the dynamics of single gas-vapor bubbles and the dynamics of the bubble ensemble created earlier at our institute were used. The models are built on a system of differential equations and describe the transfer of heat and mass through the interphase surface "liquid – steam" within the framework of molecular-kinetic theory. To calculate the dynamics of steam-gas bubbles, it is necessary to present in an analytical form an equation that adequately describes the nature of the change in external pressure due to which bubbles grow or compress. This is an equation specific to each individual problem and is a basic equation.

To carry out the experimental part of the research, acidic condensate from a boiler house in city Kyiv («Vynohradar» district) and a model liquid were used – a solution of carbon dioxide in distilled water with a pH close in size to condensate. The experiments were carried out on a laboratory stand, which consists of two main working units of a rotary – pulsation apparatus (RPA) of a special design and a thermal vacuum processing unit. The method of experimentation assumed that the processed sample of liquid with a volume of 30 liters was processed in a closed circuit in recirculation mode for 10 minutes in the absence of supply and delivery of the treated fluid. Samples were selected every minute throughout the processing cycle (10 minutes) to determine the optimal time. Sampling was carried out through a special pipe at the outlet of the tank of the thermal vacuum treatment unit.

The pH value was measured using the EZODO PCT – 407 device according to the standard methodology described in the operating rules. Simultaneously with the pH, the temperature of the condensate and model liquid was controlled. Measurements were carried out before processing, every minute for 10 minutes of processing and 7 hours after processing.

The selected samples were stored in a non-sealed polypropylene disposable container without direct sunlight.

## Results and Discussions

On the basis of universal mathematical models of dynamics of single gas-vapor bubbles created earlier in our institute and dynamics ensemble of the bubble, numerical modeling of the growth of gas-vapor bubbles in condensate was carried out. Within the framework of the mathematical model dynamics of the ensemble of bubble, an analytical study of the evolution of a totality of steam-gas bubbles until a critical value of the gas content in them is reached.

Figure 1 shows the change in the size of the gas content depending on the radius of the growing bubbles in the monodispersed ensemble.

Monodispersed aggregates of bubbles with seven values of the initial radius in the range from 0.7 microns to 10 microns at an initial concentration of carbon dioxide of 70 mg/l and a liquid

temperature of 25°C were investigated. The dotted line shows the value of the critical gas content (the ratio of the volume of the gas phase to the volume of the liquid)  $\beta_{inv} = 0.65$  at which the inversion of the flow structure occurs (the transition from the liquid-bubble structure to the gas-droplet). The figure shows that for all values of the initial radius, the radius of the bubbles increase by about five times when the critical gas content is reached. That is, the volume of the bubble phase increases by more than two orders of magnitude. Those sections of curves 1-7 that are above the dotted line do not correspond to the real state, because bubbles no longer exist in this area due to inversion of phase.

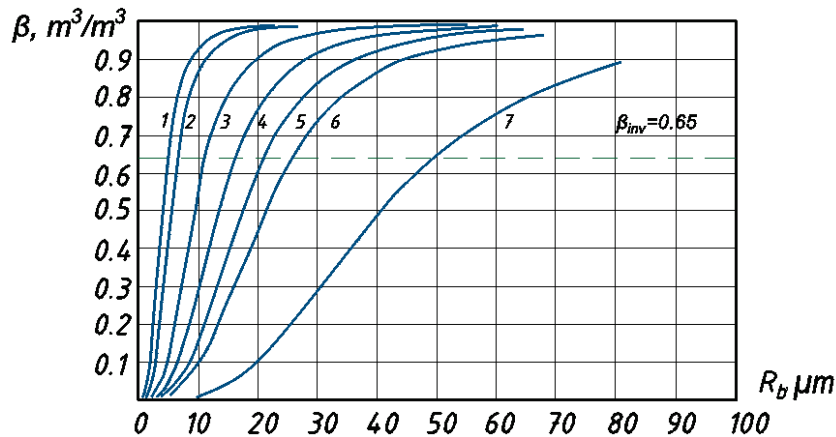


**FIGURE 1.** The dependence of the gas content of a monodisperse totality bubbles of carbon dioxide in water on their current radius at different values of the initial radius: 1 – 0.7 microns; 2 – 1 microns; 3 – 2 microns; 4 – 3 microns; 5 – 4 microns; 6 – 5 microns; 7 – 10 microns

Figure 2 shows the results of calculating the dependence of the gas content on the growth time of bubbles for nine monodispersed bubble ensembles with initial radii in the range from 0.5 microns to 5 microns at an initial concentration of carbon dioxide of 70 mg/l and a liquid temperature of 25°C. As can be seen from the figure, small bubbles with an initial radius of up to 0.6 microns do not grow at all during this mode of operation of the installation. It is characteristic that bubbles of all initial sizes from 0.7 to 5 microns reach a critical value of gas content in almost the same period of time (115÷140 μs) from the moment the external pressure drops. It is characteristic that the increase in gas content in the totality of bubbles with relatively large bubbles with an initial radius of more than 2 microns occurs slowly. While for, a totality of small bubbles with an initial radius of up to 1 micron, the gas content increases almost instantly.

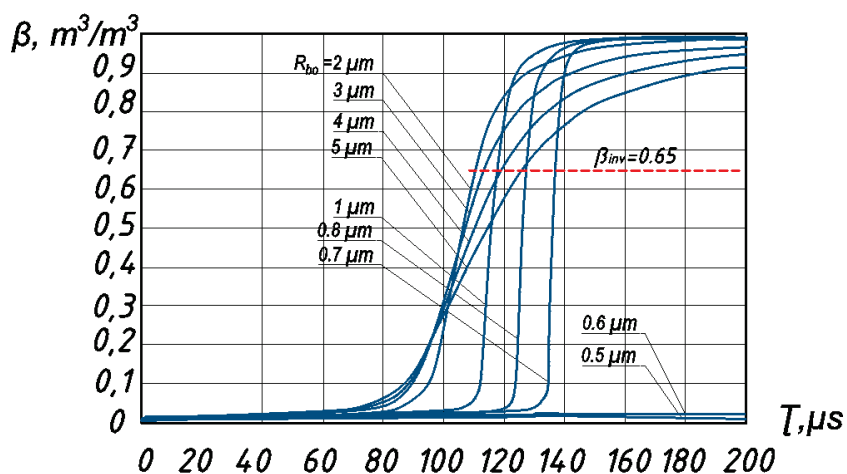


**FIGURE 2.** Change over time of the radius of the value of the gas content of the monodispersed totality of carbon dioxide bubbles in water at different values of the initial radius

These results provide useful information for further research on this problem.

As the above research results have shown, small bubbles with an initial radius of up to 0.6 microns cannot grow at all even with large pressure drops initiated during condensate processing in the proposed way. Also, this method of processing cannot lead to further grinding of microbubbles. However, when a liquid-bubble flow passes through the channels of RPA inside the apparatus, a number of powerful mechanisms are initiated, as a result of which there is a strong dynamic effect on the fluid: flow of very high stresses and shear rates (about  $2.5 \cdot 10^5 \text{ c}^{-1}$ ), periodic high-frequency pressure changes and abnormally high changes in accelerations both in direction and in magnitude, short-term micro vortices, etc. Due to the total action of these factors – high-frequency braking and acceleration of fluid, eddy formation, intensive mixing, etc., the collision of bubbles, their coagulation and the formation of larger bubbles or bubble totality are possible. Then large bubbles form already during the passage of condensate through the RPA channels.

The calculations also showed that the rate of desorption of carbon dioxide from the surface of condensate droplets during their stay at the stage of gas extraction is very small compared to the rate of release of undissolved free carbon dioxide from condensate. This is the advantage and perspective of the proposed method of neutralization.

To confirm the obtained results of numerical modeling of the process of carbon dioxide extraction from a liquid, experimental studies of changes in the pH value of condensate of natural gas combustion products were carried out.

The results of studies on the treatment of acidic condensate in the proposed way confirmed the assumption of the possibility of reducing the acidity of condensate. For comparison, model fluid was also subjected to processing.

Figure 3 shows the results of the dependence of the pH of condensate (curve 1), model fluid (curve 2) on the duration of processing and after 7 hours of holding of the treated condensate (curve 3) and model fluid (curve 5). Lines 4 correspond to the pH of degassed distilled water – 6.6 (according to DSTU ISO 3696 2003). That is, the values to which you need to seek when neutralizing condensate.

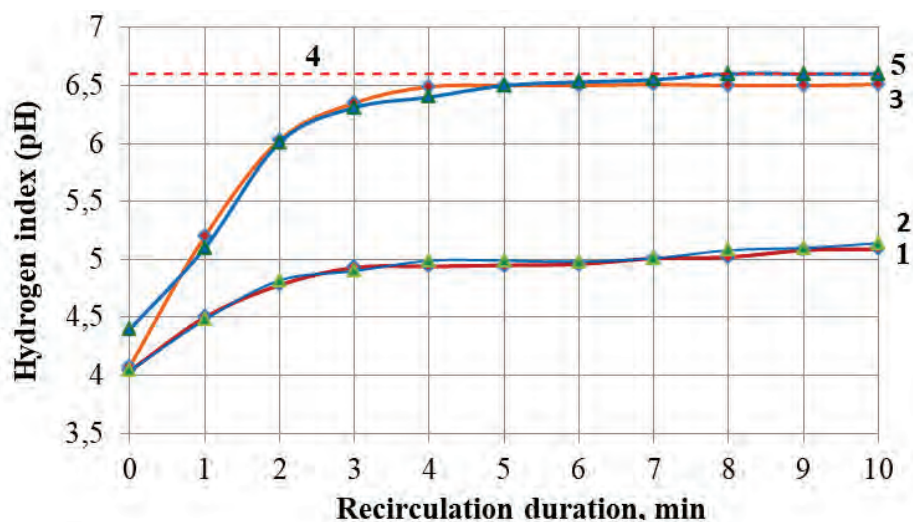


**FIGURE 3.** Dependence of the change in the pH of condensate on the duration of processing: 1 – condensate; 2 – model fluid; 3 – condensate after 7 hours of exposure; 4 – degassed distilled water; 5 – model fluid after 7 hours of exposure

The major amount of carbon dioxide is removed within 2 minutes of treatment. After 4 minutes of processing, the pH remains constant, which indicates that further processing is impractical. It was revealed that after processing the condensate is in an unstable state and its pH continues to increase, which is explained by the course of the process of liquid relaxation. After 7 hours of exposure, the pH of the condensate stabilizes at a value of 6.5, which corresponds to the almost complete absence of carbon dioxide in it.

The obtained results of the pH of condensate indicate that after processing we obtain neutralized condensate, which by physicochemical parameters is similar to desalinated water with a low content of dissolved carbonic acid.

The measurement of the change in condensate and model fluid temperature during its processing due to the dissipative release of heat was approximately 1.8°C/min, and for the working cycle 1.5±2 minutes and was insignificant. However, an increase in temperature should have a positive effect on the rate of removal of carbon dioxide from the liquid. Therefore, it is advisable to supply condensate for processing immediately after the economizer.

## Conclusion

The traditional and newest methods of neutralizing condensate, their advantages and disadvantages are briefly considered. It was established that the use of mechanisms of DPEI is promising for neutralization and degassing of condensate of natural gas combustion products.

Based on the created universal mathematical models of the dynamics of single steam-gas bubbles and the ensemble of bubble dynamics, numerical modeling of the growth of steam-gas bubbles in condensate was carried out. Within the framework of the mathematical model of the dynamics of the ensemble of bubbles, an analytical study of the evolution of the unit of steam-gas bubbles to achieve a critical value of the gas content in them was carried out.

Experimentally of way determined that the main amount of carbonic acid from the condensate of flue gases and model fluid is removed within two minutes of processing. The obtained pH values of condensate after neutralization are close to the values of distilled water at which carbonic acid is practically absent. The use of the proposed method of neutralizing condensate will create conditions for improving the environment by reducing the amount of effluent (chemically contaminated neutralized condensate and waste from water softening plants) and rational use of water resources by reducing the need for natural water.

## References

- [1] Zaporozhets A.O., Babak V.P., 2020, *Control of fuel combustion in small and medium power boilers*. Kyiv: PH "Akademperiodyka". 128 p.
- [2] Kishnevskiy V.A., Chichekin V.V., Shulyak S.D., 2011, *Application of carbonifiers in the flowsheets of water-treatment*. Proceedings of the Odessa Polytechnic University. Vol. 36, No 2, pp. 120-124 [in Russian].
- [3] Bukovska M., Novak K., Proshak-Miąsik D., Rabchak S., 2017, *Concept of Heat Recovery from Exhaust Gases*. IOP Conference Series: Mater. Sci. and Eng. 245 052057 Concept of Heat Recovery from Exhaust Gases.
- [4] Sharapov V.Y., Syvukhyna M.A., *Calciners for water treatment plants of heat supply systems*. Moscow PH "ACB", 200 p. [in Russian].
- [5] Galustov V.S., 2004, *About water decarbonization*. Akva-Term, Vol. 5, No 21, pp. 76-79 [in Russian].
- [6] Dolinskiy A.A., Ivanitsky G.K., 2008, *Heat and mass transfer and hydrodynamics in vapor-liquid dispersed media*. Physical foundations of discrete-pulse energy input. Kiev: PH "Naukova dumka". 381 p. [in Russian].

Borys BASOK<sup>1</sup>, Denys DEREVINKO<sup>1,2</sup>

Nataliia BESPALA<sup>1</sup>, Ihor BOHOIKO<sup>2</sup>

<sup>1</sup> Institute of Engineering Thermophysics of the National Academy of Science of Ukraine  
2a, Marii Kapnist (Zhelyabova) Str., Kyiv, 03057, Ukraine

<sup>2</sup> National Technical University of Ukraine "Igor Sikorsky Kyiv Polytechnic Institute"  
115, Borschahivska str., Kyiv, 03056, Ukraine

Corresponding author: e-mail: dereviankodenys@gmail.com

Doi: 10.53412/jntes-2022-2-2

## FEATURES OF COMPLEX ASSESSMENT OF ENERGY CONSERVATION MEASURES IN BUILDINGS

**Abstract:** *The paper is devoted to the complex assessment of the feasibility of energy conservation measures for buildings with the help of financial and technical indicators. The considered dynamic methods of estimation of aforementioned measures for energy efficiency increase in buildings allow to receive more exact financial indicators during a life cycle of the building. It is determined that the use of technical factors in addition to the financial indicators allow to define the optimal energy conservation measures. By optimal measures authors mean those that are most feasible and give higher technical effect in the achievement of appropriate comfort level in buildings after their renovation.*

*An algorithm for assessing the feasibility of implementing the measures to improve energy efficiency in buildings is proposed. This algorithm is based on the use of graphical models of the complex representation of technical and economic indicators. Its use helps the procedure of the analyses before the implementation of energy conservation measures.*

**Keywords:** *energy conservation measures, energy efficiency in buildings, feasibility indicators, buildings*

### Introduction

The reduction in the consumption of energy resources for heating purposes in buildings can be achieved by using [1, 2]: modern heat-insulating materials and technologies at the stages of design and operation; non-traditional and renewable energy sources (RES) and distributed generation (DG) systems; means of automatic management of heating systems of buildings; various user behavior management programs.

The sector of renewable energy is developing every year more and more, due to the reassessment of the priorities of the countries of the world. Unfortunately, global investments in RES remain at an insufficient level for a significant increase in the share of renewable energy. Record high prices for natural gas and coal led to an increase in prices for electricity and heat. Today, with the new prices for traditional energy carriers, energy from RES is becoming even more competitive in the market of generation technologies. There is a need for rapid development of solar, wind and other generation to increase the competitiveness of the energy sector. Figure 1 shows the global trends in the use of RES for heating residential and public buildings [4-6].

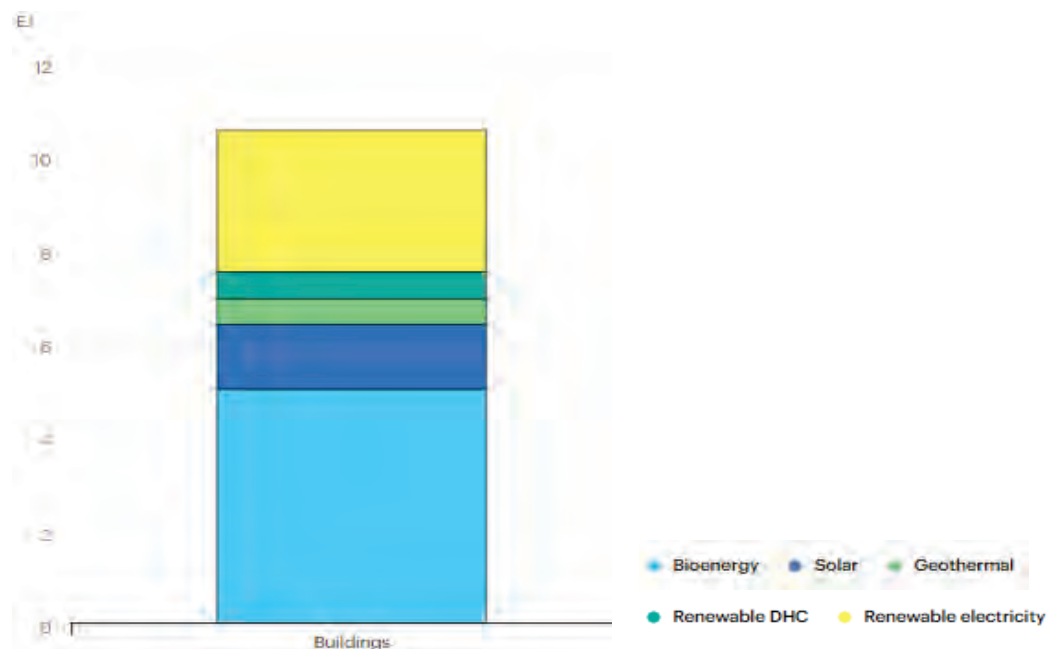


**FIGURE 1.** The share of different types of RES in the total consumption of thermal energy by buildings

When developing energy conservation measures, buildings should be considered as complex thermal energy systems, which include the internal microclimate, the building envelope, engineering networks, and the external climate. This approach makes it possible to carry out a comprehensive analysis of the energy characteristics of buildings and to implement a reasonable and efficient use of energy resources. Mathematical models can be used to assess efficiency of energy consumption at various stages of a building's life cycle. For a long time, the energy characteristics of buildings were determined for annual/seasonal calculation intervals (stationary calculation) [2, 6].

## Results

In accordance with the optimization tasks, the algorithm for determining and evaluation of the energy effects from the implementation of energy conservation measures (ECM's) to improve the energy efficiency of buildings consists of the following main stages (see Fig. 2).

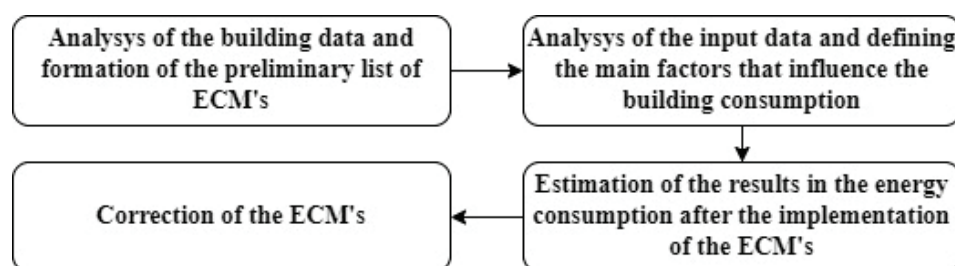


**FIGURE 2.** Algorithm for determining and evaluating of the energy effects from the implementation of measures to improve the energy efficiency of buildings

At the first stage, the initial state of the object (building) is analyzed from the point of view of data analyses and preliminary selection of a set of ECM's. For most budget facilities, it is advisable to start the analysis precisely with the possibilities of "passive" energy saving. After choosing a complex of necessary ECM's, it is necessary to identify them, including by the type of obtained energy effects [8, 10]: Energy; Economical; Ergonomic; Environmental; Financial.

Also, it is important to assess the initial conditions, determine the factors that affect the consumption of energy resources by the building. It is necessary to evaluate the initial conditions, identify and

account for influencing factors: independent variables and (or) static factors. At this stage (stage 2), a general analysis of the building's energy consumption over recent years is carried out, from the point of view of identifying the basic trend, possible fluctuations, and factors affecting the level of energy consumption are also assessed.

After forming a list of measures to improve energy efficiency at the first stages, the task of selecting the most appropriate of them, taking into account the condition of the building and other aspects of the implementation of individual measures, appears. At the same time, energy saving purposes can be obtained both by changing parameters that have a strong impact on reducing the use of energy resources, and by changing the duration of equipment operation during the year [11]. In addition, the analysis and calculation of each technical solution should be carried out for the entire life cycle from the beginning of investment in project work to the disposal of equipment.

To form an assessment of the feasibility of implementing energy-saving measures, such measures should first of all be divided into certain groups, for example: measures aimed at increasing the efficiency of an individual heating unit, increasing the thermal resistance of enclosing structures, reducing hot water consumption, increasing the frequency of air exchange.

For each of the groups, the initial energy characteristics (before the implementation of the measures) and the characteristics after the implementation of the measures are calculated. Accordingly, economic and financial indicators (NPV, NPVQ) are calculated.

The next step is the ratio of the initial and final technical factors for each energy efficiency improvement measure in each group, respectively (see Fig. 3).

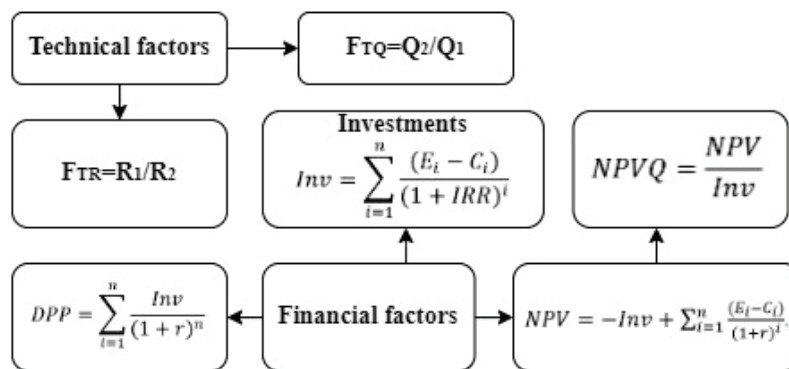


FIGURE 3. Technical and financial factors [10, 11]

Assessing the feasibility of implementing a particular ECM is carried out graphically based on two indicators – the ratio of initial and final technical parameters and the NPVQ profitability index.

On the basis of the obtained values, a diagram of the dependence of NPVQ on the value of the ratio of technical factors is constructed (Fig. 4a).

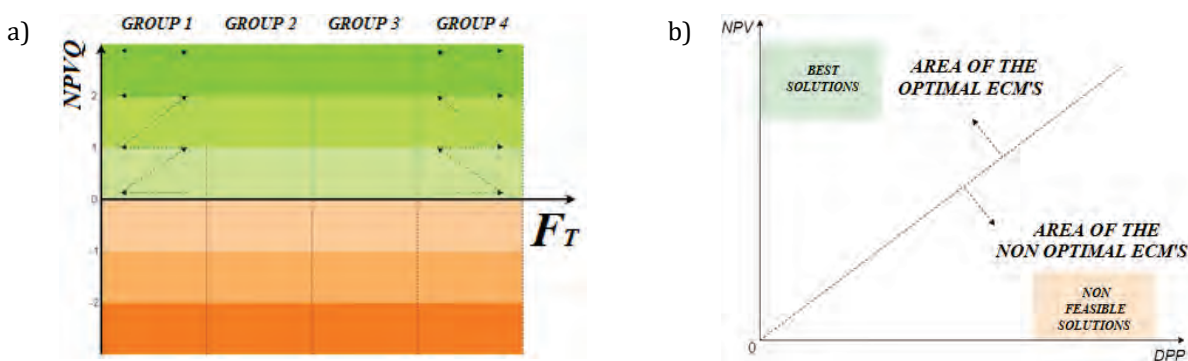


FIGURE 4. Diagram of dependence of NPVQ and factor of technical efficiency  $F_T$  (a) and diagram for comparing the effectiveness of ECM's of one group (b)

After plotting the points into the diagram corresponding to NPVQ values and the ratio of technical factors ( $F_T$ ), a matrix of points is formed that correspond to specific ECM in a certain group. By comparing the positions of the points corresponding to the ECM's relative to the coordinate axes, taking into account the specifics of the implementation of the measures and the value of the technical factors, among several measures of the same group, the one that is the most effective and, accordingly, the most expedient, is chosen.

When two or more measures fall into the zone of greatest efficiency and a choice must be made between them, it is proposed to add the dependence of NPV on the discounted payback period of DPP to the selection criteria. It is also convenient to choose between two such measures by evaluating their parameters graphically using the diagram shown in Figure 4b.

Based on the results of energy audits in buildings of the communal sphere, we will give example of calculating the value of saving energy and changing the technical characteristics of enclosing structures, engineering systems, and climatic conditions before and after the implementation of a number of measures to improve energy efficiency.

**TABLE 1.** Parameters of evaluation of building energy saving measures [9, 10, 12]

ECM group	Specific ECM	$F_T$	NPVQ	NPV, UAH	DPP, years
Increase of thermal resistance	1. Insulation of external walls	0.34	0.12	57 162.6	11.7
	2. Replacement of windows	0.84	0.07	4 560.1	12.3
Increasing the efficiency of the heating system	3. Modernization of IHP	0.067	3.10	1 726 455.7	2.7
	4. Flushing the heating system	0.91	2.7	416 546.1	2.10

The next step is the ratio of the initial and final technical factors for each ECM in each group, respectively.

The diagram (Fig. 5) graphically shows the location of the points corresponding to the measures from Table 1. Based on the position of the points, it can be concluded that measures numbered 1 and 3 in the first and second groups, respectively, will be the most appropriate for implementation.

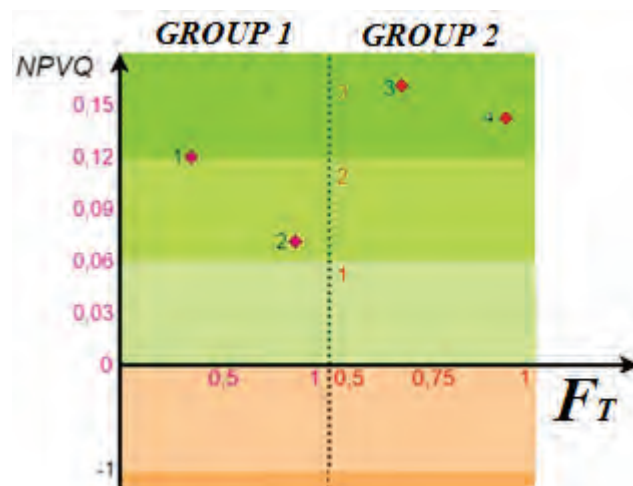


**FIGURE 5.** Diagram of the distribution of measures by the level of feasibility of their implementation

However, there are cases when it is quite difficult to draw a clear conclusion, as in the case of the measures of the second group. In such cases, it is worth applying the evaluation method using the ratio of NPV to the discounted payback period of DPP, constructing the diagram in Figure 6.

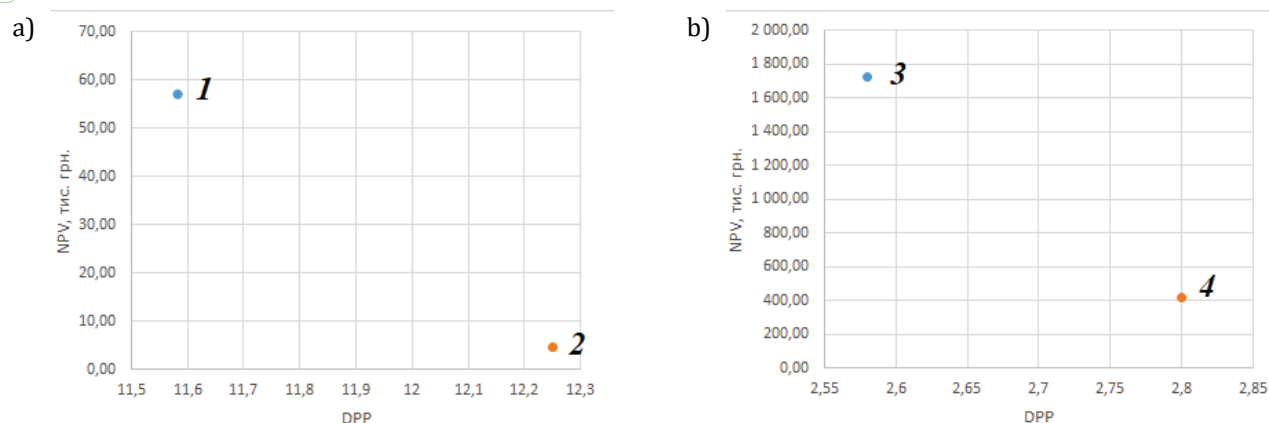


**FIGURE 6.** Comparison of measures of the thermal resistance increase group (a); groups for increasing the efficiency of the heating system (b)

Assessing the feasibility of implementing a particular measure to improve energy efficiency is carried out graphically based on two indicators – the ratio of initial and final technical parameters and the NPVQ profitability index. Therefore, after analyzing the indicators of the above measures, the most effective in this case is the modernization of the IHU.

## Conclusions

The considered dynamic methods of assessing the expediency of implementing measures to improve energy efficiency in communal buildings make it possible to more accurately assess financial indicators during the life cycle of the building. Technical factors should also be taken into account along with economic factors. The algorithm proposed in this work for assessing the feasibility of implementing measures to improve energy efficiency in communal buildings makes it possible to comprehensively evaluate technical and economic indicators when analyzing individual ECM's. This algorithm is based on the application of graphic models of complex presentation of technical and economic indicators. Therefore, its use will help to make a decision on the implementation of exactly such measures to improve energy efficiency, which will allow not only to save money, pay off investments, but also to increase the level of comfort of staying in buildings and to reach the level of minimum requirements of current legal acts.

## References

- [1] On energy efficiency: Law of Ukraine of 17 December. 2020 №4507. URL: [http://w1.c1.rada.gov.ua/pls/zweb2/webproc4\\_1?pf3511=70687](http://w1.c1.rada.gov.ua/pls/zweb2/webproc4_1?pf3511=70687) (access date: 21.10.2021).
- [2] Dodonov B., *Energy Efficiency Monitoring of Ukraine 2015*. URL: [https://www.ua.undp.org/content/ukraine/uk/home/library/environment\\_energy/energy\\_efficiency\\_ukraine2015.html](https://www.ua.undp.org/content/ukraine/uk/home/library/environment_energy/energy_efficiency_ukraine2015.html).
- [3] Ministry of Energy and Coal Industry of Ukraine, NEC Ukrenergo, Scientific and Technical Center of Electric Power Industry. Analysis of energy efficiency in developed foreign countries and dependence on their imports. URL: [https://ua.energy/wp-content/uploads/2018/01/1.-Efektyvnist\\_energ\\_resursiv.pdf](https://ua.energy/wp-content/uploads/2018/01/1.-Efektyvnist_energ_resursiv.pdf).
- [4] International Renewable Energy Agency. URL: <https://www.irena.org/>.
- [5] International Energy Agency. URL: <https://www.iea.org>.
- [6] Derevianko D., 2022, *Peculiarities of determination of economic indicators of executibility of implementation of measures to increase energy efficiency*. Derevianko D., Kolodiazhna A., Nytsun Y. POWER ENGINEERING: economics, technique, ecology. No. 1, pp. 38–45. – ISSN 1813-5420. DOI 10.20535/1813-5420.2.2021.247412.
- [7] Decree of the President of Ukraine on the Sustainable Development Strategy "Ukraine - 2020". URL: <https://zakon.rada.gov.ua/laws/show/5/2015#Text>.

- [8] DIRECTIVE 2009/125 / EC OF THE EUROPEAN PARLIAMENT AND OF THE COUNCIL of 21 October 2009 on a framework for the setting of ecodesign requirements for energy-using products (new version). URL: [https://zakon.rada.gov.ua/laws/show/984\\_011-09#Text](https://zakon.rada.gov.ua/laws/show/984_011-09#Text).
- [9] Order of the Cabinet of Ministers of Ukraine of November 25, 2015 № 1228-r On the National Action Plan on Energy Efficiency until 2020. URL: <https://zakon.rada.gov.ua/laws/show/1228-2015-%D1%80#Text>.
- [10] Training manual for local government officials. Energy efficiency in the municipal sector. URL: <https://enecities.org.ua/upload/files/3energoefweb%281%29.pdf>.
- [11] Ministry of Energy and Coal Industry of Ukraine NEC Ukrenergo Scientific and Technical Center of Electric Power Industry. Legislative and regulatory incentives to increase the efficiency of energy use in leading foreign countries. URL: <https://ua.energy/wp-content/uploads/2017/05/1.Zakonodavche-stymulyuvannya-energoefektyvnosti.pdf>.
- [12] Law of Ukraine on Energy Conservation. Information of the Verkhovna Rada of Ukraine (VVR), 1994, № 30, p. 283. URL: <https://zakon.rada.gov.ua/laws/show/74/94-%D0%B2%D1%80#Text>.

Oleksandr SIGAL, Dmytro PADERNO, Nataliia NIZHNYK

*Laboratory of thermophysics processes in boilers,*

*Department of heat-physical problems of heat supply systems*

*of the Institute of Engineering Thermophysics of the National Academy of Sciences of Ukraine*

*2A, M. Kapnist str., Kyiv, 03057, Ukraine*

Corresponding author: sigal@engecology.com

Doi: 10.53412/jntes-2022-2-3

## POSSIBILITIES FOR THE PRODUCTION AND USE OF HYDROGEN AS A FUEL IN EXISTING BOILERS

**Abstract:** *The process scheme is developed for climate neutral production and use of hydrogen as a fuel in existing boilers at heat supply enterprises.*

**Keywords:** *hydrogen, municipal solid waste, incineration*

**Abbreviations:** *MSW – municipal solid waste, RDF – refuse derived fuel*

Using of hydrogen at present is a key priority to achieve the European Green Deal and Europe's clean energy transition [1], and application of it as a fuel for at least partial replacement of the fossil fuels is one of the essential components to support the EU's commitment to reach carbon neutrality by 2050 and for the global effort to implement the Paris Agreement while working towards zero pollution [2].

In spite of the obvious environmental advantages, such using creates a number of currently unresolved problems due to the peculiarities of the hydrogen characteristics as a fuel, which stipulates the necessity for changing of the modes of its combustion, of the construction of fire chambers, heat-receptive elements, etc. The problems for hydrogen practical use in combustion processes in the existing boiler equipment are pointed out in [3], and maybe the main problem is that the adiabatic hydrogen combustion temperature in air is high, about 260° higher than the adiabatic combustion temperature of usually used natural gas.

However, this peculiarity may be quite useful for processes where the combustion temperature is usually insufficiently high, and must be increased.

Such a process is, in particular, the thermal processing of the municipal solid waste (MSW).

The world's leading countries consider solid waste as an alternative local energy resource that is constantly generated and is very convenient logistically – in populated areas, close to energy consumers.

At present in Ukraine, especially under conditions of military aggression against our country, one of the largest threats to national security is Ukraine's energy dependence on imported natural gas; reducing of this dependence is a priority task for ensuring the stable operation of Ukraine's energy system. The special State targeted economic program for the energy recovery of MSW at enterprises – heat energy producers is now under development in Ukraine, the purpose of which is to attract the energy potential of MSW due to its energy recovery to the country's energy balance, as well as to solve the problem of sanitary cleaning of cities due to the utilization of a significant share of MSW.

According to the EU legislation [4], which is now under implementation to the Ukrainian legislation, waste incineration plants shall be designed, equipped, built and operated in such a way that the

temperature of combustion even under the most unfavourable conditions must be kept at least at 850°C for at least two seconds.

With taking into account the quite low calorific value of usual MSW (about 1650 kcal/kg) and even of the Refuse derived fuel (RDF) made from MSW (2000-4000 kcal/kg), keeping of such temperature often requires an additional high calorific fuel.

The possible solution is using the hydrogen as such additional fuel. The proposed process for realizing this technique is schematically presented at Figure 1.

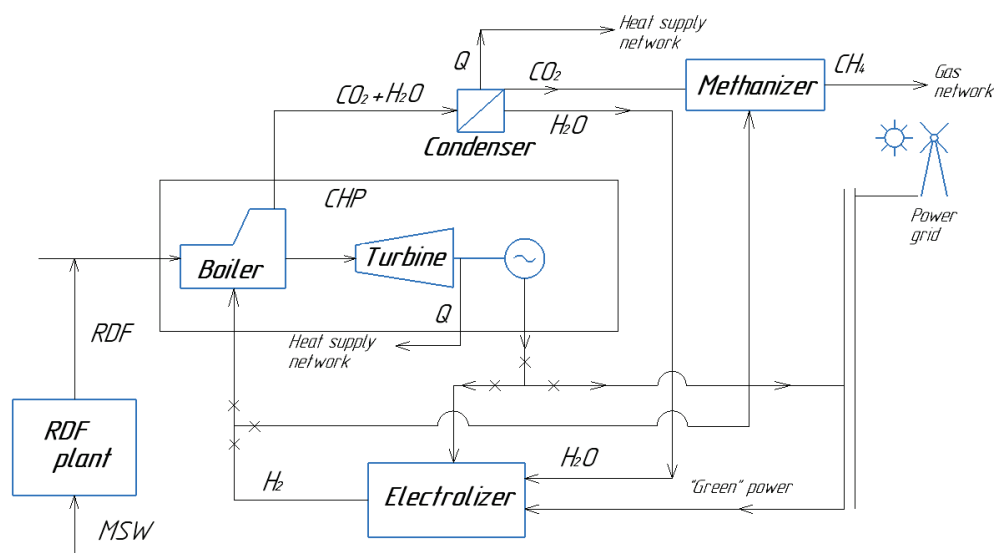


FIGURE 1. Process scheme for using hydrogen at waste incineration

Hydrogen is generated by electrolysis with using “green” power from renewable sources (solar, wind, etc.) or own produced at the CHP, and is fed partly to the fire chamber of boiler combusting RDF, causing increasing of the combustion temperature, and partly is fed to the methanizer.

The water vapour contained in flue gases is condensed to liquid water, and carbon dioxide is fed to the methanizer.

During the reaction of interaction of hydrogen with carbon dioxide from flue gases of boilers, synthetic methane is formed in the methanizer, the formed methane-hydrogen mixture (up to 10% hydrogen) may be used practically as the usual methane, in particular may be used in existing natural gas firing boilers, or fed to a local natural gas network.

The carbon dioxide formed during the subsequent burning of such a mixture is no longer counted as a greenhouse gas emission.

The above process idea is at the stage of obtaining a patent.

Such process is proposed by the authors for implementation in the heat supply schemes for cities of Kyiv (at the heat supply station ST-1) and Odesa (at the region boiler-house Pivdenna-1), developed with participation of the authors.

## References

- [1] The European Green Deal. URL: [https://ec.europa.eu/info/strategy/priorities-2019-2024/european-green-deal\\_en](https://ec.europa.eu/info/strategy/priorities-2019-2024/european-green-deal_en).
- [2] Communication from the commission to the European parliament, the council, the European economic and social committee and the committee of the regions. A hydrogen strategy for a climate-neutral Europe. URL: <https://eur-lex.europa.eu/legal-content/EN/TXT/?uri=CELEX:52020DC0301>.
- [3] Nizhnyk N., Sigal A., Plashykhin S., Safiants A., 2022, *Influence of hydrogen on the toxic substances formation process during co-incineration with natural gas*. International Science Journal of Engineering & Agriculture. Vol. 1, No. 4, pp. 19-26. doi: 10.46299/j.isjea.20220104.05.

Dagmara KOTRYS-DZIAŁAK, Katarzyna STOKOWIEC

Kielce University of Technology

al. Tysiąclecia Państwa Polskiego 7, 25-314 Kielce, Poland

Corresponding author: ddzialak@tu.kielce.pl

Doi: 10.53412/jntes-2022-2-4

## TEMPERATURE DISTRIBUTION ANALYSIS ON THE SURFACE OF THE RADIATOR WITH AN INFRARED CAMERA AND THERMOCOUPLES

**Abstract:** *The aim of the work was to perform experimental tests for thermal analysis on the outer surface of the radiator. For this purpose, a localized test stand was used in one of the lecture rooms in Kielce University of Technology. The experiment concerned the isothermal character of a radiator during its operation. Temperature distribution was verified with two different methods: thermocouples and thermovision camera. The radiator was divided into 8 measuring fields and temperature was measured in each of them. The experiments were conducted for different supply flow rates of the medium. The results were presented by means of diagrams comparing both methods of temperature survey.*

**Keywords:** radiator, thermal analysis, isothermal, thermovision, thermocouples

### Introduction

Most of us spend plenty of our every day time in the buildings interiors. We sleep, spend some of our free time and even often work inside different types of rooms. One of the most important factors during that time is our general sensation named as thermal comfort and defined by ASHRAE (ASHRAE, 2013) as: “the condition of mind in which satisfaction is expressed with the thermal environment”. In order to analyze the function between the surrounding environment and the person thermal comfort a proper balance was required and the predicted mean vote (PMV) index has been proposed by Fanger model. The scale ranges between -3 to +3 depending on the cold or hot conditions. The approach includes the heat transfer between the occupant and his environment (Stokowiec et al., 2022). The environmental parameters are: air temperature, mean radiant temperature, relative humidity and air velocity. As it can be concluded, the temperature inside the room (both air and radiant ones) strongly influences our sensations.

That is why in order to predict the personal thermal feelings, it is necessary to conduct experiments on the source of proper temperature level inside the room. When analyzing winter season, the heating season in particular, the heating system is of key importance. The elements that transfer the heat to the room interior are heaters. Depending on the heating media they can be water/steam/electric or gas ones. On the other hand, we can divide heaters to convection, that principle is the motion of heated air, or radiant ones, that heat the surfaces around. The materials used for their production are cast iron, aluminum or steel. They can be manufactured as plate, of tinned tubes or sectional radiators.

Many investigations have been conducted in order to observe the phenomena occurring in the area of the operating radiators that influence the personal comfort system in order to extend acceptable comfort zones. Results from the survey conducted in China revealed (Du et al., 2020) that the feet and lower body parts were the most preferred parts to be heated in winter and therefore local heating

device was designed to supply warm air to subjects' feet and calves directly. For the experiments 20 subjects (10 males and 10 females) were randomly recruited.

Radiant heating was also compared to other systems such as all-air systems (Karmann et al., 2017) and in that case they provide equal or even better thermal comfort. In case of convective and radiant heating systems, there was no significant thermal comfort difference observed (Lin et al., 2016). Radiant electric heaters that are situated overhead provide localized heat in case of historic buildings (churches) without affecting painted walls or works of art that are displayed (Samek et al., 2007). Radiant heaters are most commonly used in case of any large-cubage building. However, they can be also gas-fired with the possibility of additional heat energy recovery from the flue gases of gas radiant heaters (Dudkiewicz and Szałański, 2019).

The temperature stratification was much higher during research of convective heaters compared to floor heating system, but still not significant enough to change the thermal comfort vote. The reduction of temperature stratification can be achieved by means of heating from the floor and cooling from the ceiling (Causoen et al., 2010). The opposite situation results in high discomfort due to the great temperature stratification (d'Ambrosio Alfano et al., 2014). Moreover, the air temperature stratifications depending on the heating systems may differ: during the experiment the convector achieved the worst air temperature stratification (Legera et al., 2018).

The tests were also conducted for radiant temperature distribution patterns generated by radiant heaters with different power outputs and suspended at different angles (Dudkiewicz and Jezowiecki, 2011). The results refer to parameters characterizing the thermal comfort of people in large capacity halls. Other research analyzed the heat enhancement by means of additional coatings or mesh structures (Chatys and Orman, 2017; Dąbek et al., 2019).

The studies of radiant panel heater evaluated the perception of indoor environment and investigated experimentally the comparison with conventional portable natural convective heaters, resulting with the conclusion that situating the panel heaters on the wall facing the window and on the wall close to the window, provides the best operative temperature distribution in the office room (Ali and Morsy, 2010).

Numerous examinations have been performed on convective-radiative heat transfer: the effect of turbulence has been modelled (Wang et al., 2014) indicating that the ratio between convection and radiation is directly proportional to the Grashof number and inversely to the surface emissivity. Turbulent natural convective energy transport above a heated element phenomenon has also been conducted statistically, dividing turbulent flow into three regions according to power spectrum distribution analysis (Zhang et al., 2016). The research also noted that the enclosure geometry presents high impact on determining the circulation configuration and heat transmission inside the enclosure (Miroshnichenko and Sheremet, 2018).

The underfloor heating system is also widely analyzed and described in the literature. The studies mainly are grouped in two fields: the economic analysis (Karimi et al., 2019) or experimental and numerical research of system design and performance (Magni et al., 2019). Recently, the interested has grown in the aspect concerning the energy transport and liquid circulation (Stepan et al., 2021).

Both not enough theoretical and experimental analyzes have been recently performed in order to research the convection heaters as an element of a central heating system in the building. The studies include the estimation of preheating time in case of buildings that are not continuously occupied, such as shopping malls, office buildings, and residential houses (Sun et al., 2022). Thermal analysis based on the obtained experimental laboratory results was used to assess the heating efficiency of heaters with parameters: different power consumption, geometric shape and dimensions (Bertolin et al., 2015).

The environmental protection issues, including the reduction of carbon dioxide and other pollutants emissions, involve the thermomodernization practices (Wciślik, 2017) with the energy efficiency of the heating system and economic analyzes required.

Due to the scarce scientific and academic achievements evaluating the convection heaters, the paper presents thermal study with the experimental results of convection heaters incorporated in the

laboratory installation simulating the real central heating system operation. The scope of the experiments was to measure the isothermal field of the heaters.

## Methodology

### *Conducted research and the testing device*

The research was taken during the heating period season in November in one of the lecture rooms in Energis – a laboratory and didactic building that is an intelligent, self-sufficient and modern part of Kielce University of Technology complex. The tested installation consists of hydraulic system with an electric boiler as a heat source, radiators, pumps, heating pipes with all necessary equipment such as: shut off valves, regulating valves, and others as shown in Figure 1. The system simulates the central heating operation on one outlet, and the domestic hot water on the other.



**FIGURE 1.** Lecture room in Kielce University of Technology with tested installation

To carry out the research one of the four panel radiators was connected to the DaqLab2000 data acquisition station using 8 thermocouples. The station collected the changes of the temperature on the surface of the tested radiator with dedicated computer software program. DaqLab2000 is a measurement system by IOtech equipped with an ethernet interface. The device allows the measurement of analog signals (8 channels, 16 bit converter/200 kHz), frequency measurements (4 channels, 16 bit/10 MHz). Additionally, the user gets 6 digital inputs/outputs available (+24 on DB37 connector).

In the same time infrared camera Testo 890 was located opposite the measured radiator (Fig. 1) and several thermograms were taken during the heating process. For each of the four supply flow rates that were set during the experiment, the measurements lasted for 4.5 minutes with a 15 seconds interval. Thermal imaging camera used in the research has a resolution of 640×480 pixels, with the SuperResolution technology of 1280×960 pixels. Its thermal sensitivity is <math><40\text{ mK}</math> which allows to see even the smallest temperature differences. Temperature measuring range is from

During the experiment the electric boiler was set to the

dedicated for this type of radiator. The heater is made of cold-rolled steel sheet in accordance with PN-EN 10130 and is painted with white colour RAL 9016. The max. working pressure is 10 bar, and max. working temperature is 100°C.

The front panel of the radiator was divided into 9 fields and on 8 of them thermocouples were located according to the Figure 2.

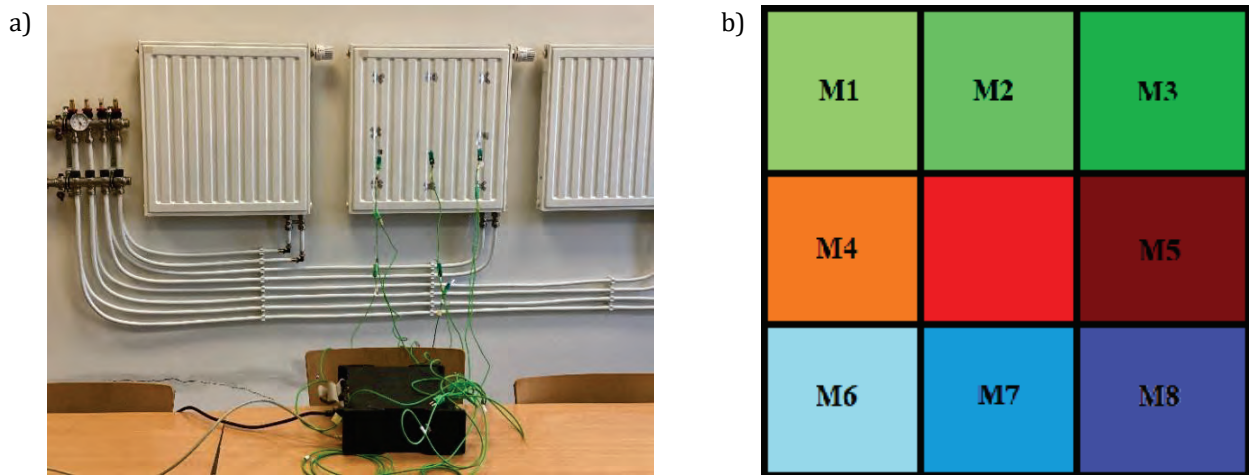


**FIGURE 2.** Tested Radiator with 8 no. field measurement location: a) actual photo, b) arrangement of the measured fields

Emissivity of the tested object was tested in the beginning of the experiment by using tape of known emissivity and defined as 0.92. That factor was applied into THV camera during the experiment. The glossy surface of the heater and thus the reflection of radiation from surrounding objects was not include.

### Results and discussion

Based on the results obtained from the measurement series for both THV camera and thermocouples, temperature distribution as a function of flow rate is shown in Figures 3, 4 and 5 depending on the location of the measuring points of the radiator (top, middle and bottom).

As shown in Figure 3 the points M2 and M3 located at the top of the radiator are with the highest temperature according to measurements with thermocouples and according to infrared camera. The mean temperature of the surface of the radiator rises with the flow rate. The M3 and M2 points are the closest points to main vertical channel that distributes the water inside the radiator and are the highest values. The differences in temperatures between the M3 and M1 points are between 0.74°C and 1.3°C with thermocouples and 0.36°C and 1.02°C respectively with infrared camera.

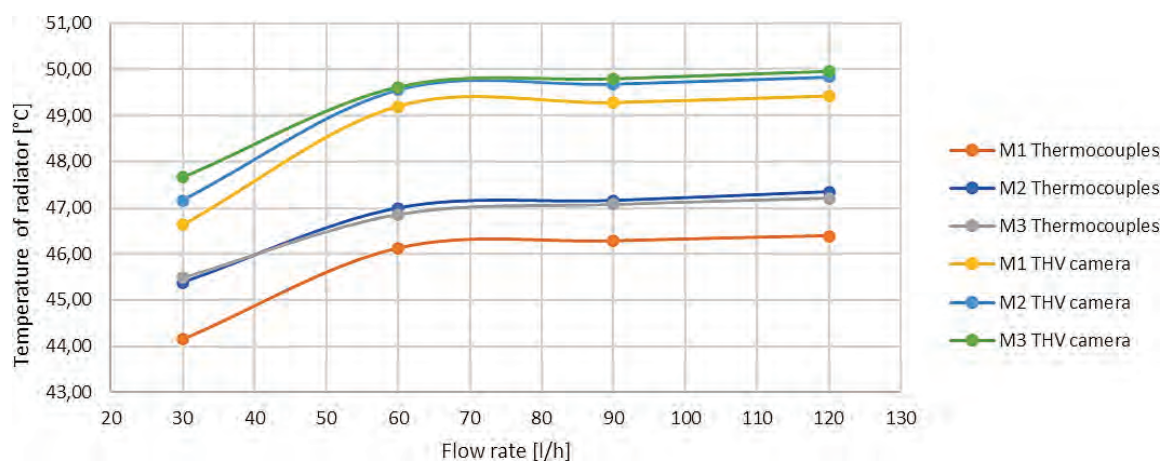


**FIGURE 3.** Temperature distribution in upper part of the radiator as a function of flow rate

In the middle part of the radiator only two fields were measured with thermocouples, the M4 point is located at the left side of the heater and M5 on the opposite end, therefore the difference in temperature between the two is greater and is around  $1^{\circ}\text{C}$  with the min. and max. values of  $0.74^{\circ}\text{C}$  and  $1.15^{\circ}\text{C}$  respectively (Fig. 4).

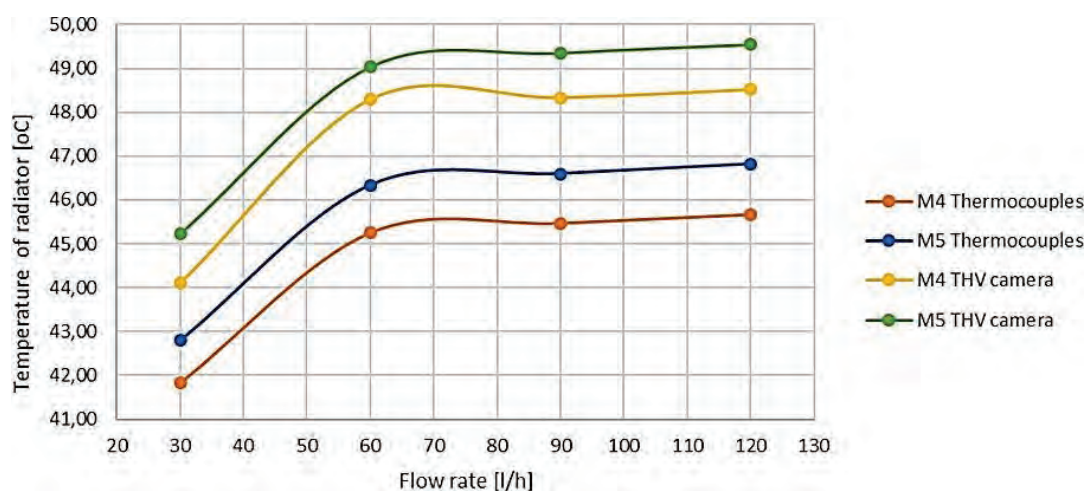


FIGURE 4. Temperature distribution in middle part of the radiator as a function of flow rate

Figure 5 represents the bottom part of the examined heater which is the coolest area in the radiator according to the research that took place. The temperature changes between the M8 and M7 and M6 is greater than in the middle part and is in range from  $0.55^{\circ}\text{C}$  to  $2.19^{\circ}\text{C}$ . The temperature differences between the points are lower according to thermovision camera then thermocouples, despite the higher temperature rates achieved by infrared camera.

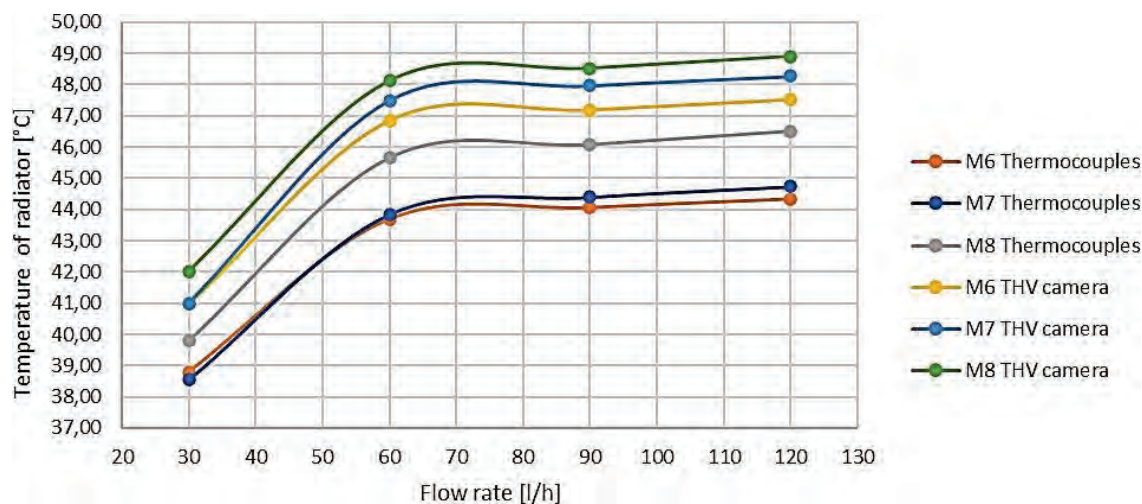


FIGURE 5. Temperature distribution in bottom part of the radiator as a function of flow rate

The mean values were calculated for all three parts of the radiator that were tested and Figure 6 represents the results. The distribution analysis show that the surface is not isothermal despite the applied method. The greater the flow rate the changes in temperature difference are smaller, but with its minimum flow rate  $30\text{ l/h}$  value the  $dT$  is even  $5.96^{\circ}\text{C}$  with thermocouples and  $5.82^{\circ}\text{C}$  with infrared camera between the fields (regarding the mean values for each of the part studied). The overall mean temperature surface of the radiator is  $44.92^{\circ}\text{C}$  and  $47.66^{\circ}\text{C}$  for each of the research method. Standard deviation for the mean temperatures depending on difference flow rates was calculated as 2.32 in terms of thermocouples and 2.43 regarding infrared camera experiment. Figure 7 illustrates characteristics of temperature difference between the two measurement method for each of the 8 points and show that the temperature difference between is significant and at some points it reaches even  $dT\ 3.65^{\circ}\text{C}$ .

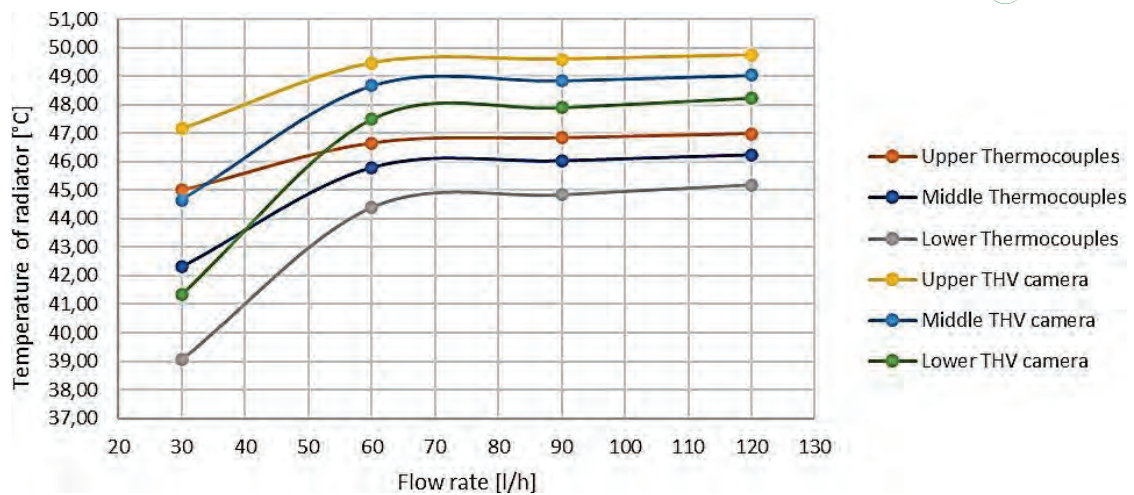


FIGURE 6. Mean temperature distribution in top, middle and bottom part of the radiator as a function of flow rate

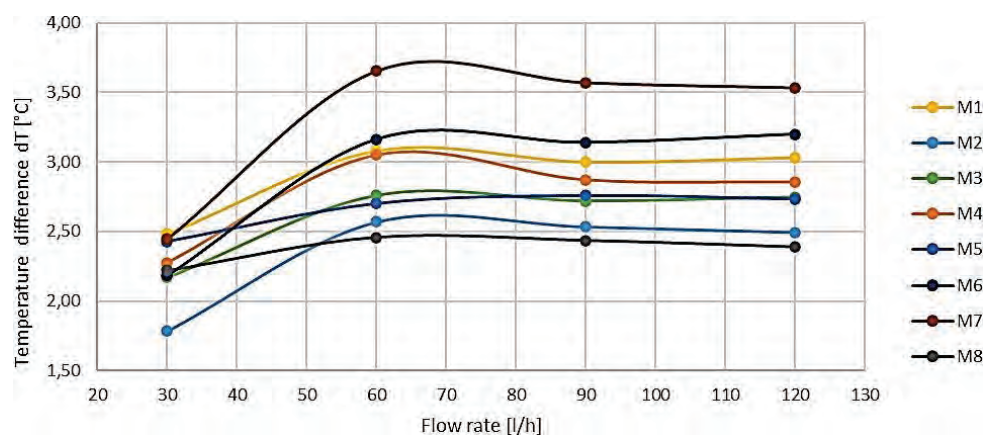


FIGURE 7. Characteristics of the temperature difference between the thermocouples and the themovision camera measurements for M1 to M8

Temperature change over time is shown in Figure 8 and Figure 9 for THV camera and thermocouples respectively. As noticed on both of the diagrams temperature increases equivalently with the flow. The highest temperature during the entire experiment was noted in points M3, M2 and M5 for each of the method. The curves were prepared for water flow of 120 l/min, which was the final test taken. The diagrams proof the non-isothermal temperature distribution on the heater, even thou the radiator was heated and the max flow rate was achieved.

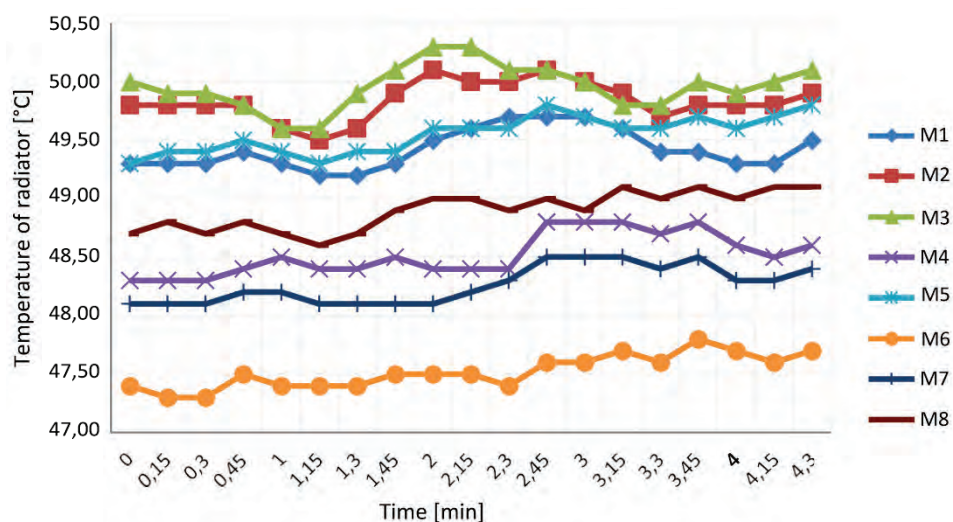


FIGURE 8. Temperature change for 8 points M1 to M8 for 120 l/min water flow with infrared camera measurements

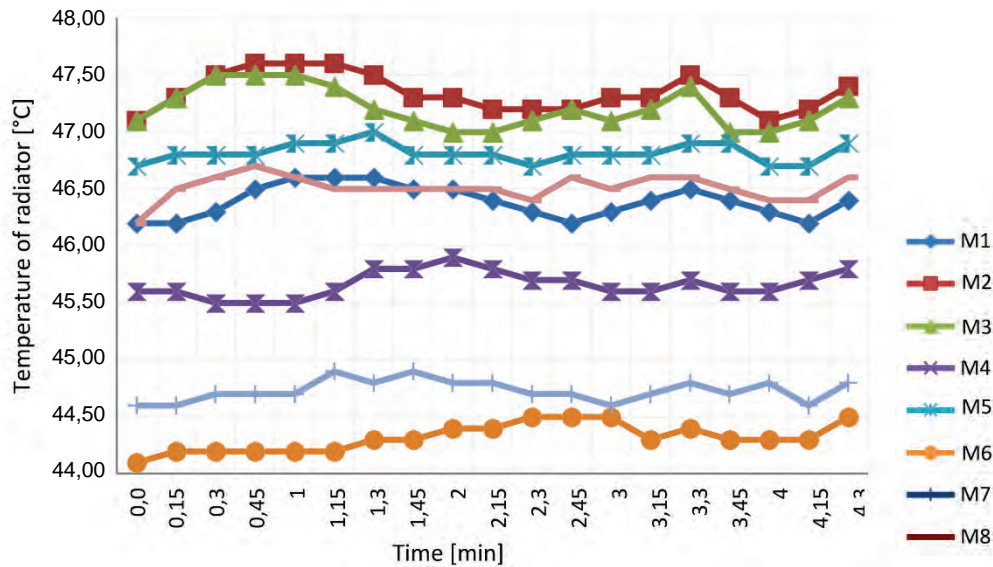


FIGURE 9. Temperature change for 8 points M1 to M8 for 120 l/min water flow with thermocouples measurements

Using thermograms the infrared camera show how temperature fields are shaped. Figure 10 is an example thermogram taken at the flow rate of 30 l/h and at 120 l/h, the reddish colors show the hottest temperatures and the green and blue the coldest.

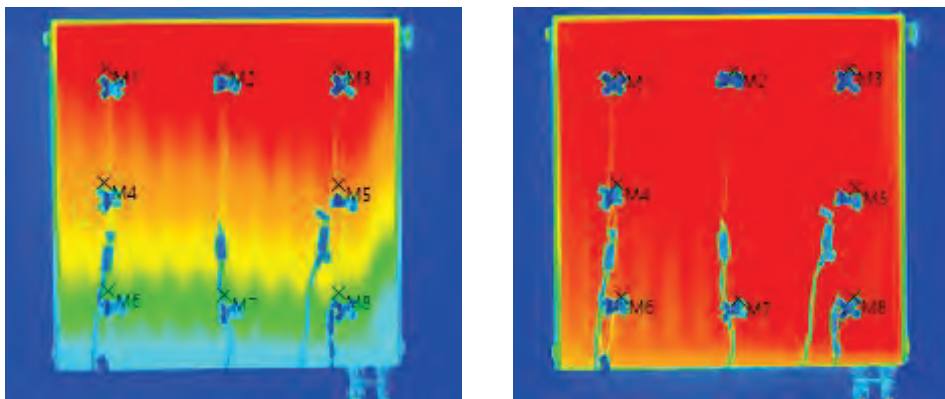


FIGURE 10. Thermogram of a radiator showing measured fields (M1 to M8) with 30 l/h and 120 l/h of flow rate

The connection of the radiator to the hydraulic system right side bottom has a huge impact on the temperature distribution especially with the min flow rate required by the radiator. The right side of the radiator and also its upper side is warmer and is heated much faster than the rest of the radiator. This has a huge impact on the process of convection, and affects the thermal comfort of the occupants inside the environment. During the whole process internal air temperature was monitored and the temperature increased from 23.6°C to 25.5°C with the max. flow rate of 120 l/h. The outside air temperature was around 10°C.

## Conclusion

Between the two methods the infrared camera and thermocouples there are differences in temperatures of top, middle and bottom part of the radiator with the min. of 1.78°C and max. of 3.65°C differences. The contact method with thermocouples and acquisition station seems to be more accurate. The thermovision method despite the camera accuracy and the examined emissivity factor have given highest temperatures. There are numerous reasons for that. One of them is the distance between the object and the infrared camera. The other one is the direct sun light that appear during the experiment and the room was not fully shaded. The mechanical ventilation and floor heating systems installed in the

room could have increased the surface temperature of the panel heater. Based on the conducted study, further analysis of the measurement uncertainty of the devices can be performed as well as thermal comfort analysis of the occupants with the radiators as a main source of heating.

## References

- Ali A.H.H., Morsy M.G., 2010, *Energy efficiency and indoor thermal perception: a comparative study between radiant panel and portable convective heaters*, Energy Efficiency, 3, pp. 283-301.
- ASHRAE-55, Thermal Environment Conditions for Human Occupancy, ASHRAE, 2013.
- Bertolin C., Luciani A., Valisi L., Camuffo D., Landi A., Del Curto, D., 2015, *Laboratory tests for the evaluation of the heat distribution efficiency of the Friendly-Heating heaters*, Energy and Buildings, 107, pp. 319-328.
- Causone F., Baldin F., Olesen B.W., Corgnati S.P., 2010, *Floor heating and cooling combined with displacement ventilation: possibilities and limitations*, Energy Building, 42, pp. 2338-2352.
- Chatys R., Orman Ł.J., 2017, *Technology and properties of layered composites as coatings for heat transfer enhancement*, Mechanics of Composite Materials, 53 (3), pp. 351-360.
- d'Ambrosio Alfano F.R., Olesen B.W., Palella B.I., Riccio G., 2014, *Thermal comfort: design and assessment for energy saving*, Energy Building, 81, pp. 326-336.
- Dąbek L., Kapjor A., Orman Ł.J., 2019, *Distilled water and ethyl alcohol boiling heat transfer on selected meshed surfaces*, Mechanics & Industry, 20, 701.
- Du C., Liu H., Li C., Xiong J., Li B., Li G., Xi Z., 2020, *Demand and efficiency evaluations of local convective heating to human feet and low body parts in cold environments*, Building and Environment, 171, 106662.
- Dudkiewicz E., Jezowiecki J., 2011, *The influence of orientation of a gas-fired direct radiant heater on radiant temperature distribution at a work station*, Energy and Buildings, 43, pp. 1222-123.
- Dudkiewicz E., Szałański P., 2019, *A review of heat recovery possibility in flue gases discharge system of gas radiant heaters*, E3S Web of Conferences 116, 00017.
- Karimi M.S., Fazelpour F., Rosen M.A., Shams M., 2019, *Comparative study of solar- powered underfloor heating system performance in distinctive climates*, Renewable Energy, 130, pp. 524-535.
- Karmann C., Stefano S., Bauman F., 2017, *Thermal comfort in buildings using radiant vs. all- air systems: a critical literature review*, Building Environment 111, pp. 123-131.
- Légera J., Rouse D.R., Le Borgne K., Lassue S., 2018, *Comparing electric heating systems at equal thermal comfort: An experimental investigation*, Building and Environment, 128, pp. 161-169.
- Lin B., Wang Z., Sun H., Zhu Y., Ouyang Q., 2016, *Evaluation and comparison of thermal comfort of convective and radiant heating terminals in office buildings*, Building Environment, 106, pp. 91-102.
- Magni M., Campana J.P., Ochs F., Morini G.L., 2019, *Numerical investigation of the influence of heat emitters on the local thermal comfort in a room*, Building Simulation, 12, pp. 395-410.
- Mikhailenko S.A., Miroshnichenko I.V., Sheremet M.A., 2021, *Thermal radiation and natural convection in a large-scale enclosure heated from below: Building application*, Building Simulations, 14, pp. 681-691.
- Miroshnichenko I.V., Sheremet M.A., 2018, *Turbulent natural convection heat transfer in rectangular enclosures using experimental and numerical approaches: A review*, Renewable and Sustainable Energy Reviews, 82, pp. 40-59.
- Samek L., De Maeyer-Worobiec A., Spolnik Z., Bencs L., Kontozova V., Bratasz Ł., Kozłowski R., Van Grieken R., 2007, *The impact of electric overhead radiant heating on the indoor environment of historic churches*, Journal of Cultural Heritage, 8, pp. 361-369.
- Stokowiec K., Kotrys-Działak D., Jastrzębska P., 2022, *Verification of the Fanger model with field experimental data*, Journal of Physics: Conference Series, 2339, 012027.
- Sun S., Xing X., Wang J., Sun X., Zhao C., 2022, *Preheating time estimation in intermittent heating with hot-water radiators by considering model uncertainties*, Building and Environment, 226, 109734.
- Wang Y., Meng X., Yang X., Liu J., 2014, *Influence of convection and radiation on the thermal environment in an industrial building with buoyancy-driven natural ventilation*. Energy and Buildings, 75, pp. 394-401.
- Zhang X., Yu J., Su G., Yao Z., Hao P., He F., 2016, *Statistical analysis of turbulent thermal free convection over a small heat source in a large enclosed cavity*, Applied Thermal Engineering, 93, pp. 446-455.
- Wciślik S., 2017, *Energy efficiency and economic analysis of the thermomodernization of forest lodges in the Świętokrzyski National Park*, EPJ Web of Conferences 143, 02144.

Viacheslav MYKHAILYK, Tetiana KORINCHEVSKA

Valery DAKHNENKO

*Institute of Engineering Thermophysics of National Academy of Sciences of Ukraine*

*2a, Marii Kapnist Str., Kyiv, 03057, Ukraine*

Corresponding author: mhlk45@gmail.com

Doi: 10.53412/jntes-2022-2-5

## TORREFACTION OF COMPOSITE BIOFUEL IN THE ATMOSPHERE OF ITS OWN GASEOUS ENVIRONMENT

**Abstract:** *Torrefied pellets of composite fuel made from a mixture (1:1) of pine wood with lowland peat and pine wood were studied by TGA and DTA methods. Torrefaction was carried out at atmospheric pressure in a gaseous environment, which was formed in a limited space during the partial thermal decomposition of organic substances of fuel. An increase in the torrefaction temperature from 250 °C to 290 °C leads to an increase in the degree and temperature range of fuel decomposition. The presence of wood in the composite fuel has a positive effect on the results of torrefaction: the heat of thermal decomposition increases, ash content and hydrophilicity decrease. The method of torrefaction without the use of inert gases has shown its effectiveness and the possibility of application in the production of torrefied fuel.*

**Keywords:** *torrefaction, thermal decomposition, composite granular fuel, pine wood, peat*

### Introduction

At peat deposits in Ukraine, actively used for many years, the ash content often exceeds the standard established for peat as a fuel [1]. Its thermal characteristics can be improved by creating a composite with plant materials [2] and by performing granulation. However, this does not solve the problems of high hydrophilicity and biological damage. The use of biofuels and peat in energy sector requires a more significant increase in calorific value and the creation of conditions for effective dispersion.

Torrefaction is among the well-known methods of increasing the energy properties of biofuel. It is a thermochemical process in an inert or limited oxygen environment, where the biomass is slowly heated to a predetermined temperature and maintained for a specified time [3, 4].

The main components of plant biomass are hemicellulose, cellulose and lignin. Coniferous wood contains 48-56% cellulose, 26-30% lignin, and 23-26% hemicellulose [5]. These components are much less in lowland type peat. The total content of hemicellulose and cellulose residues in it is on average about 27.6%, and 12.3% lignin. However, peat contains ~40.2% humic acids, ~15.5% fulvic acids, and ~4.2% bitumen [6].

The temperature range of torrefaction is from 200°C to 300°C [7-9]. During torrefaction, most of the hemicellulose and amorphous cellulose decomposes, while crystalline cellulose and lignin undergo less decomposition [10-12]. Thermal destruction is accompanied by a change in the composition of biomass, a loss of ~40% of mass and 10-15% of energy [3, 13]. The content of low-calorie components decreases [14] and the content of cellulose and lignin increases, the calorific value of which is much higher [15]. As a result of torrefaction, the carbon content increases, which leads to an increase in the heat of combustion of the fuel [16, 17].

Another important aspect of the torrefaction conditions is the oxygen concentration in the reactor. It was found [11] that the presence of a small amount of oxygen has a beneficial effect on the course of the process. During torrefaction biomass loses its fibrous structure, becomes brittle, grinds easily, and does not lose its properties to form granules without auxiliary binders [18, 19]. Due to the destruction of OH groups, the fuel loses its hydrophilicity. This simplifies the conditions for its transportation and storage and provides protection against biological degradation [3]. Torrefaction makes it possible to bring the properties of the fuel as close as possible to the properties of thermal coal and to burn it in pulverized coal boilers [3, 4, 7].

The creation of an inert environment complicates and increases the cost of torrefaction technology. Therefore, it is relevant to study the possibility of carrying out the torrefaction process in a gaseous atmosphere, which occurs in a limited volume during the thermal decomposition of organic fuel substances.

### Materials and methods

Pellets from a mixture (1:1) of lowland peat and crushed pine wood (composite fuel), 8 mm in diameter and 30-40 mm long, were subjected to torrefaction. Pine wood pellets were also made for comparison. The torrefaction took place at atmospheric pressure in a non-hermetic steel cylindrical container with a volume of 0.5 l, which was densely filled with pellets. Heating was carried out in a muffle furnace (Fig. 1). The temperature of the furnace and pellets in the container was registered using thermocouples and a DT821A controller. The wires of the thermocouples were inserted into the container through a small hole, which simultaneously served as a channel for the exit of excess gases formed during the torrefaction process. The container was placed in a muffle furnace preheated to 250°C, 270°C or 290°C. The countdown of the torrefaction time was started after the pellets reached the furnace temperature. The torrefaction time was 60 min at a temperature of 250°C and 290°C and 30 min at 270°C (Fig. 2).

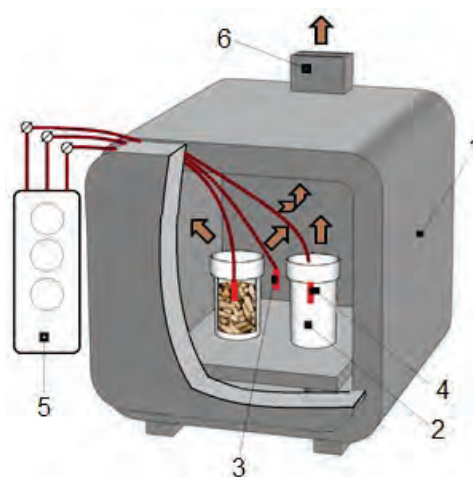


**FIGURE 1.** Equipment for torrefaction: 1 – muffle furnace; 2 – container; 3, 4 – temperature sensors; 5 – controller; 6 – nozzle for exhaust gases

Thermal analysis of fuels was carried out in the derivatograph "Q-1000" of the Paulik-Paulik-Erdey system ("MOM" company, Hungary), modernized in the Institute of Engineering Thermophysics (IET) of National Academy of Sciences of Ukraine, in the range of 20-1000°C at a sample heating rate of 7.4 K/min. The temperature scale was corrected according to the transition temperature of quartz from  $\alpha$ - to  $\beta$ -form (573°C). The temperature deviation did not exceed  $\pm 0.5$  K. The collection and processing of information from the measurement channels of the derivatograph was carried out using applied computer program "Derivatograph", created at IET. Fuel samples crushed in a porcelain mortar were loaded into a conical alundum crucible. An inert substance (aluminum oxide) was in the comparison crucible.

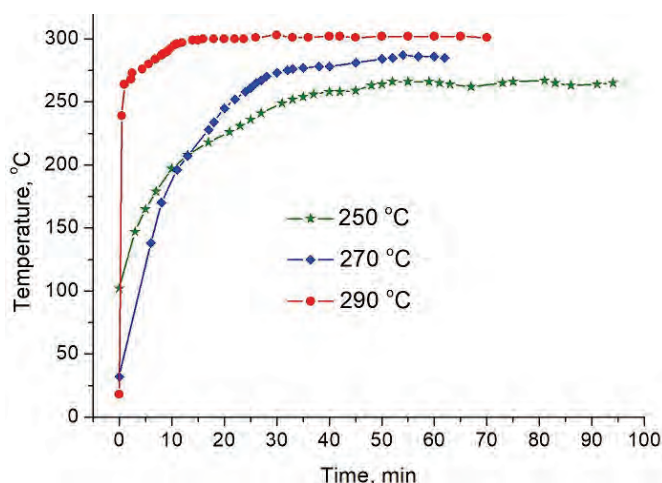


FIGURE 2. Temperature change of composite fuel pellets during torrefaction at furnace temperatures of 250°C, 270°C, and 290°C

### Measurement results and discussion

The degree of decomposition and the yield of torrefied fuel were calculated from the data on the change in the mass of the pellets during heat treatment. Table 1 show that under the same conditions, pellets made of wood acquire a higher degree of decomposition compared to pellets of composite fuel.

TABLE 1. The degree of decomposition of granulated biofuel and the yield of torrefied fuel

Temperature in the furnace, °C	Torrefaction time, min	Degree of decomposition, %		Yield of torrefied fuel, % dry mass	
		Wood	Composite	Wood	Composite
250	60	17.06	14.62	82.94	85.38
270	30	22.98	17.64	77.02	82.36
290	60	44.64	37.62	55.36	62.38

Samples of initial fuels, the derivatograms of which are shown in Figures 3a and 3b, were subjected to thermal analysis to compare the torrefaction results. DTG and DTA curves shows that bound water is removed from wood in the range of 20-170°C and from composite fuel in the range of 20-178°C [20].

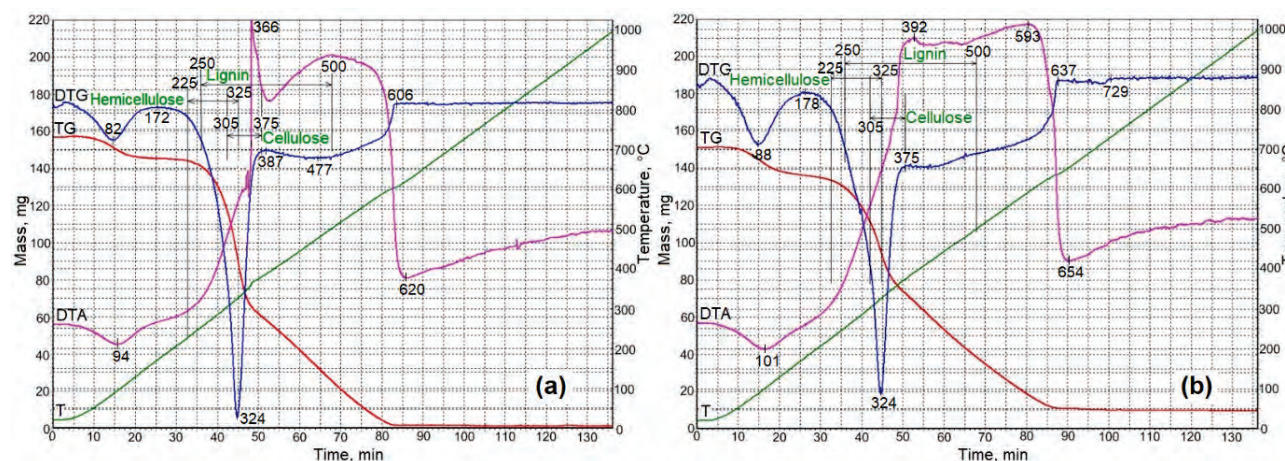


FIGURE 3. Derivatograms of pine wood (a) and composite fuel (b)

Thermal decomposition of organic substances is accompanied by a sharp change in mass and active gas formation. This is registered on the TG and DTG curves. This process reaches its maximum rate at 324°C for both fuels. However, the active phase of gas evolution in composite fuel ends at a lower temperature (375°C) than in wood (387°C).

The obtained derivatograms of the initial fuels confirm the multi-stage nature of their destruction due to the different thermal stability of biopolymers. Thermal decomposition of pine wood is completed at 606°C, and composite fuel at 637°C. Heat release (DTA curves) stops after complete thermal decomposition of organic substances after 17 K (at 654°C) for composite fuel and after 14 K (at 620°C) for pine wood due to different heat capacity and thermal conductivity of fuel residues (ash).

An endothermic process of thermal dissociation of  $\text{CaCO}_3$  (DTA curve) is observed in the composite fuel after the complete decomposition of organic substances in the range of 637-729°C (DTG curve).  $\text{CaCO}_3$  is present in peat in the form of remains of shells of molluscs.

The analysis of the derivatograms showed that the temperature of the beginning of thermal decomposition in torrefied fuels (Figs. 4 and 5) shifts towards higher temperatures compared to non-torrefied fuel (Fig. 3), and the higher the temperature of torrefaction, the greater the shift. For pine wood, it shifts from 172°C in the initial fuel to 218°C in the torrefied at 290°C (DTG curves in Figs. 3a, 4a and 4b). Under the same conditions for composite fuel, the temperature of the beginning of thermal decomposition shifts from 178°C to 207°C (DTG curves in Figs. 3b, 5a, and 5b). The increase in thermal stability is a consequence of the destruction of thermolabile components, primarily hemicellulose.

Torrefied fuel has a wider temperature range of thermal decomposition. In wood torrefied at 250°C (DTG curve, Fig. 4a), thermal decomposition is observed in the range of 203-674°C, while in the initial wood (DTG curve, Fig. 3a) destruction begins at 172°C and ends at 606°C. An increase in the torrefaction temperature shifts the temperature of the end of thermal decomposition to higher temperatures (up to 785°C in wood torrefied at 290°C) (DTG curve, Fig. 4b).

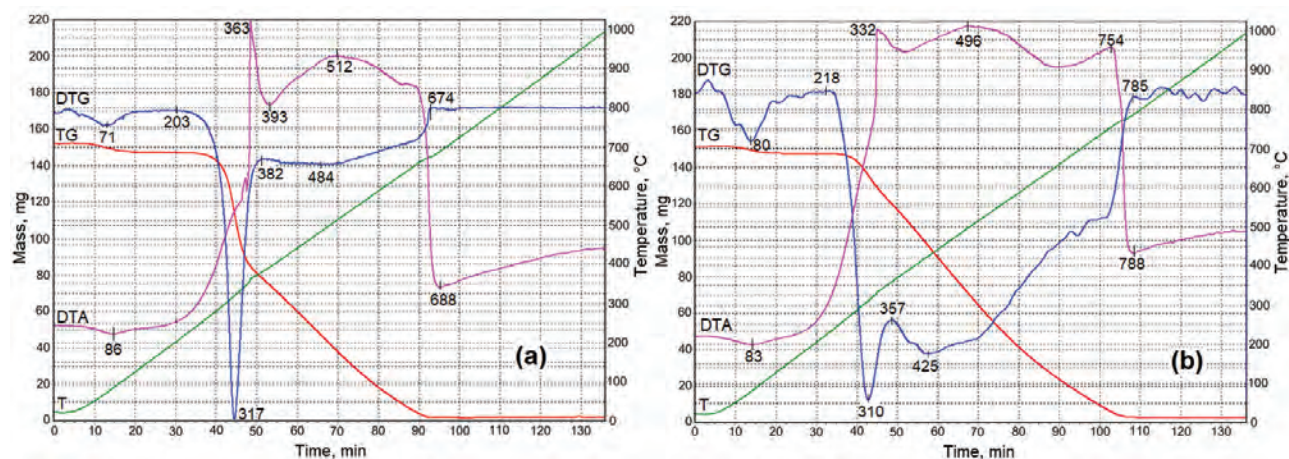


FIGURE 4. Derivatograms of pine wood after torrefaction at 250°C (a) and 290°C (b)

The temperature interval of thermal decomposition of initial composite fuel is in the range of 138-637°C (Fig. 3b). Increasing the heat treatment temperature from 250°C to 290°C increases the temperature range of its decomposition from 205-718°C to 207-767°C (Figs. 5a, 5b and 6b). Extending the range and increasing the thermal decomposition temperature indicates an increase in the carbon content in the fuel.

Figures 6a and 6b clearly show how the temperature range of heat release changes during the thermal decomposition of biofuels with a change in temperature and time of torrefaction.

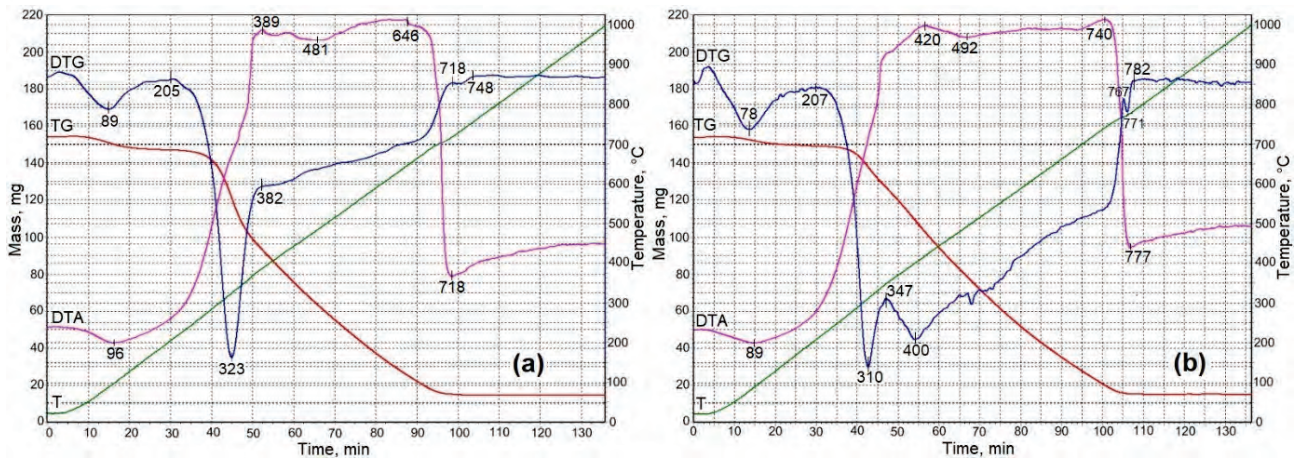


FIGURE 5. Derivatograms of composite fuel after torrefaction at 250°C (a) and 290°C (b)

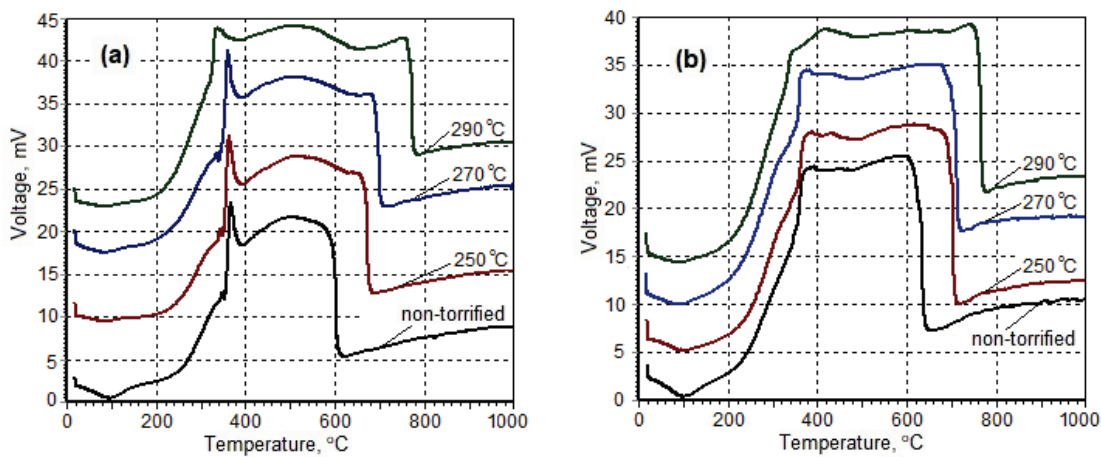


FIGURE 6. DTA curves of pine wood (a) and composite biofuel (b) before and after torrefaction at 250°C, 270°C, and 290°C

Calculations based on the TG and DTG data (Table 2) showed that the degree of decomposition (the thermally decomposed part of the dry mass of the sample related to the mass of the dry material) up to 300°C (the final temperature of the samples during torrefaction over 290°C) is 16.86% in the initial wood, and 17.51% in composite fuel. Another ~20% of wood and ~13% of composite fuel decomposes in the range from 300°C to 325°C. That is, the degree of decomposition of the initial samples of pine wood increases to 36.82% and of composite fuel to 30.32% when heated to 325°C.

TABLE 2. The degree of decomposition of the dry mass of fuels at the moment of reaching 300°C and 325°C (determined by TGA)

Fuel	Determination temperature, °C	Degree of decomposition, %	
		Pine wood pellets	Composite fuel pellets
Non-torrefied	300	16.86	17.51
	325	36.82	30.32
Torrefied at: 250°C	300	7.81	6.81
	325	27.17	17.35
270°C	300	6.27	7.74
	325	24.90	18.41
290°C	300	4.89	4.83
	325	11.42	10.61

The degree of decomposition of torrefied fuel, determined by TGA at the moment the sample reaches 300°C (Table 2), decreases by 2.92% in wood samples and by 1.98% in composite fuel with an increase in heat treatment temperature from 250°C to 290°C. This indicates an insignificant residue of hemicelluloses in the torrefied fuel. Increasing the heat treatment temperature to 325°C leads to a sharp increase in the degree of decomposition. Necessity in this mode can be determined only as a result of comparing the thermal characteristics of the obtained fuels.

Comparison of the degree of decomposition (Tables 1 and 2) shows that the degree of decomposition of biofuels during torrefaction is more than two times higher than that determined by TGA results when the samples reach 300°C. This indicates the role of the atmosphere and heat treatment time in torrefaction technology.

Torrefaction caused an increase in the hydrophobicity of fuels, which was manifested in a decrease in equilibrium moisture content (Table 3) as a result of the destruction of biopolymers and a decrease in the number of hydrophilic active centers. The equilibrium moisture content of pellets torrefied at 250°C is more than two times lower than that of non-torrefied ones. Increasing the torrefaction temperature to 290°C leads to deeper changes in the composition and structure of biofuels, which leads to an increase in their hydrophobicity. The equilibrium moisture content of composite fuel pellets is somewhat higher than wood pellets in both non-torrefied and torrefied states due to the presence of peat.

**TABLE 3.** Thermal characteristics of fuels

Fuel	Moisture content, %	Ash content, % to dry mass	Heat effect, mV·s/mg dry mass	Increase in thermal effect, %
Composite fuel pellets				
Non-torrefied	9.94	6.92	369.7	-
Torrefied at: 250°C	4.55	9.87	426.8	15.4
270°C	4.60	8.63	442.3	19.6
290°C	3.06	10.01	484.9	31.2
Pine wood pellets				
Non-torrefied	7.33	0.76	325.3	-
Torrefied at: 250°C	3.16	1.43	389.1	19.6
270°C	3.20	1.35	413.1	27.0
290°C	2.65	1.84	535.0	64.5

Ash content of torrefied fuel is higher compared to non-torrefied fuel due to unchanged mineral composition and a decrease in dry mass. A decrease in the dry mass of the fuel also leads to an increase in the ash content in it with an increase in the heat treatment temperature (Table 3).

The heat of thermal decomposition was estimated according to the method described in [2]. An estimate showed that the used torrefaction modes cause an increase in the heat of decomposition (Table 3). Thus, the specific heat of thermal decomposition of torrefied pine wood increases from 19.6% to 65.4% compared to non-torrefied wood with an increase in the torrefaction temperature from 250°C to 290°C. The specific heat of thermal decomposition of composite fuel increases from 15.4% to 31.2% under the same conditions of torrefaction (Table 2). The decrease in the thermal effect of decomposition for composite fuel is associated with peat, the torrefaction conditions of which still need to be studied. Considering that the thermal decomposition of biofuels in the derivatograph takes place in the air atmosphere, there is a direct relationship between the specific heat of thermal decomposition and the calorific value of the fuel.

The time of heat treatment affects the results of torrefaction. It can be seen from the thermal analysis data (Tables 1 and 3) that heat treatment at 270°C for 30 min is insufficient. The obtained results on the degree of decomposition, equilibrium moisture, ash content and heat of decomposition are either worse or the same as for fuel torrefied at 250°C for 60 min. The DTA curves (Figs. 6a and 6b) also show that the temperatures of the end of heat release during the thermal decomposition of torrefied fuel at 250°C and 270°C coincide.

The obtained torrefied fuels have the properties of a brittle solid. They are easily crushed to a powdery state, which is the key to effective dispersion in ball or hammer mills of power plants.

## Conclusions

Thermal analysis of torrefied pellets made from a mixture (1:1) of pine wood with lowland peat and pine wood showed that the degree of their decomposition directly depends on the temperature and time of heat treatment.

The specific heat of thermal decomposition of torrefied biofuels depends on the degree of decomposition of fuels. Pine wood pellets showed 2 times increase in the specific heat of decomposition compared to composite fuel pellets under equal torrefaction conditions. This fact requires future studies of peat torrefaction conditions.

Biofuel significantly loses its hydrophilic properties as a result of heat treatment. This is manifested in a decrease in its equilibrium moisture. Ash content of torrefied fuel increases due to a decrease in dry mass.

Studies of the method of torrefaction of biofuels at atmospheric pressure in a gaseous environment formed during the partial thermal decomposition of organic substances have shown its effectiveness and the possibility of application without the use of inert gases.

## References

- [1] *Instruktsiia iz zastosuvannia Klasyfikatsii zapasiv i resursiv korysnykh kopalyn derzhavnoho fondu nadr do torfovykh rodovyshch*, zatverdzhena nakazom Derzhavnoi komisii Ukrainy po zapasakh korysnykh kopalyn pry Derzhavnomu komiteti pryrodnykh resursiv Ukrainy vid 25.10.2004 No 224, available: <https://zakon.rada.gov.ua/laws/show/z1418-04#Text>.
- [2] Mykhailyk V.A., Snezhkin Yu.F., Korinchuk D.M., 2014, *Termichne rozkladannia hranul palyva na osnovi torfu ta derevyny*. Promyslova teplotekhnika. 36(2), pp. 11-19.
- [3] Tumuluru J.S., Sokhansanj S., Hess J.R., Wright C.T., Boardman R.D., 2011, *A review on biomass torrefaction process and product properties for energy applications*. Industrial Biotechnology. 7(5), pp. 384-401. <https://doi.org/10.1089/ind.2011.7.384>.
- [4] Granados Morales D., 2017, *Studies of the Torrefaction of Sugarcane Bagasse and Poplar Wood*, thesis. Universidad Nacional de Colombia, Sede Medellín Facultad de Minas, Escuela de Procesos y Energía.
- [5] Maryandyishev P.A., Popova E.I., Chernov A.A., Lyubov V.K., 2016, *Izotermicheskoe issledovanie drevesnogo topliva i ego organicheskikh komponentov*. Vestnik Cherepovetskogo gosudarstvennogo universiteta. 2, pp. 15-18.
- [6] *Torf*. Wikipedia, the free encyclopedia, available: <https://uk.wikipedia.org/wiki/%D0%A2%D0%BE%D1%80%D1%84>.
- [7] Shafizadeh F., 1985, *Pyrolytic reactions and products of biomass*, in: Overend R.P., Milne T.A., Mudge L.K. (Eds.), *Fundamentals of Biomass Thermochemical Conversion*.: Elsevier, London, pp. 183-217.
- [8] Basu P., 2013, *Torrefaction*, in: Basu P. (Ed.), *Biomass Gasification, Pyrolysis and Torrefaction*, second ed. Academic Press, Boston. pp. 87-145. <https://doi.org/10.1016/B978-0-12-396488-5.00004-6>.
- [9] Ciolkosz D., Wallace R., 2011, *A review of torrefaction for bioenergy feedstock production*. Biofuels, Bioprod. Bioref. 5, pp. 317-329. <https://doi.org/10.1002/bbb.275>.

- [10] Bergman P.C.A., Boersma A.R., Zwart R.W.R., Kiel J.H.A., 2005, *Torrefaction for biomass co-firing in existing coal-fired power stations "Biocoal"*, Report ECN-C-05-013. Petten, The Netherlands, Energy Research Center of the Netherlands.
- [11] Prins M.J., Ptasinski K.J., Janssen F.J.J.G., 2006, *Torrefaction of wood Part 1. Weight loss kinetics*. J. Anal. Applied Pyrolysis. 77, pp. 28-34. <https://doi.org/10.1016/j.jaap.2006.01.002>.
- [12] Prins M.J., Ptasinski K.J., Janssen F.J.J.G., 2006, *More efficient biomass gasification via torrefaction*. Energy. 31, pp. 3458-3470. <https://doi.org/10.1016/j.energy.2006.03.008>.
- [13] Phanphanich M., Mani S., 2011, *Impact of torrefaction on the grindability and fuel characteristics of forest biomass*. Bioresource Technology. 102, pp. 1246-1253. <https://doi.org/10.1016/j.biortech.2010.08.028>.
- [14] Arias B., Pevida C., Feroso J., Plaza M.G., Rubiera F., Pis J.J., 2008, *Influence of torrefaction on the grindability and reactivity of woody biomass*. Fuel Process Technol. 89, pp. 169-75. <https://doi.org/10.1016/J.FUPROC.2007.09.002>.
- [15] Medic D., Darr M., Shah A., Potter B., Zimmerman J., 2012, *Effects of torrefaction process parameters on biomass feedstock upgrading*. Fuel. 91, pp. 147-154. DOI:10.1016/j.fuel.2011.07.019.
- [16] Kim D., Park K.Y., Yoshikawa K., 2017, *Conversion of Municipal Solid Wastes into Biochar through Hydrothermal Carbonization*, in: Huang W. (Ed.), Engineering Applications of Biochar, IntechOpen, London. <https://doi.org/10.5772/intechopen.68221>.
- [17] Byichkov A.L., Denkin A.I., Tihova V.D., Lomovskiy O.I., 2014, *Raschet teplotyi sgoraniya lignotsellyulozyi na osnovanii dannyih elementnogo analiza*. Himiya rastitelnogo syirya. 3, pp. 99-104. DOI:10.14258/jcprm.1403099.
- [18] Ermochenkova M.G., Evstigneev A.G., 2017, *Izmenenie teplotyi sgoraniya drevesnogo topliva pri torrefikatsii*. Lesnoy vestnik / Forestry bulletin, 21 (1), pp. 64-68. DOI: 10.18698/2542-1468-2017-1-64-68.
- [19] Muafah A.A., Khalik M.S., Yoshimitsu U., Lukman I.A., 2012, *Study on Torrefaction of Oil Palm Biomass*. Journal of Applied Sciences. 12(11), pp. 1130-1135. <https://dx.doi.org/10.3923/jas.2012.1130.1135>.
- [20] Mykhailyk V.A., Snezhkin Yu.F., Dmitrenko N.V., 2015, *Investigation of the State of Water in Energy Trees in the Process of Drying by Differential Scanning Calorimetry*. Journal of Engineering Physics and Thermophysics. 88(5), pp. 1093-1099. <https://doi.org/10.1007/s10891-015-1288-1>.